FINAL
IN-92-CR
P.76
OCIT
67514

ORIGINAL CONTAINS
COLOR ILLUSTRATIONS
3

SPDE

Solar Plasma Diagnostic Experiment

Final Contract Report
to
The National Aeronautics and Space Administration

Contract NAS5-32147

Period of Performance
1 November, 1993 through 30 September, 1995

M. E. Bruner
Principal Investigator

Lockheed-Martin Palo Alto Research Laboratories

Contents

List of Figures

SOLAR PLASMA DIAGNOSTIC EXPERIMENT

FINAL CONTRACT REPORT
Contract NAS5-32147

Period of Performance
1 November, 1993 through 30 September, 1995

M. E. Bruner
Principal Investigator

1 Introduction

The subject of this investigation is the study of the physics of the Solar Corona through the use of high resolution soft X-ray spectroscopy and high resolution ultraviolet imagery. The investigation includes the development and application of a flight instrument, first flown in May, 1992 on NASA sounding rocket 36.048. A second flight, NASA sounding rocket 36.123, took place on 25 April, 1994. Both flights were successful in recording new observations relevant to the investigation. The investigation has been supported under several contracts, including NAS5-2-9181, NAS5-25727, HAS5-29739, the last of which ended on 31 October, 1993. The present contract (NAS5-32147) began on 1 November, 1993, at which time the SPDE instrument package was being re-configured for the second flight. The effort in this contract covers completion of the modifications to the existing rocket payload, its reflight and the preliminary data reduction and analysis.

Experience gained from flight 36.048 led us to plan several payload design modifications. These were made to improve the sensitivity balance between the UV and EUV spectrographs, to improve the scattered light rejection in the spectrographs, to protect the visible light rejection filter for the Normal Incidence X-ray Imager instrument (NIXI), and to prepare one new multilayer mirror coating for the NIXI. We also investigated the addition of a brassboard CCD camera to the payload to test it as a possible replacement for the Eastman type 101-07 film used by the SPDE instruments, as this film is no longer being manufactured. (The brassboard camera was developed under Lockheed's Independent Research Program at no cost to this contract.) This camera was included in the experimenter's data package for the Project Initiation Conference for the flight of NASA Mission 36.123, held in January, 1994, but for programmatic reasons was deleted from the final payload configuration. The payload was shipped to the White Sands Missile Range on schedule in early April. The launch and successful recovery took place on 25 April, in coordination with the Yohkoh satellite and a supporting ground-based observing campaign.

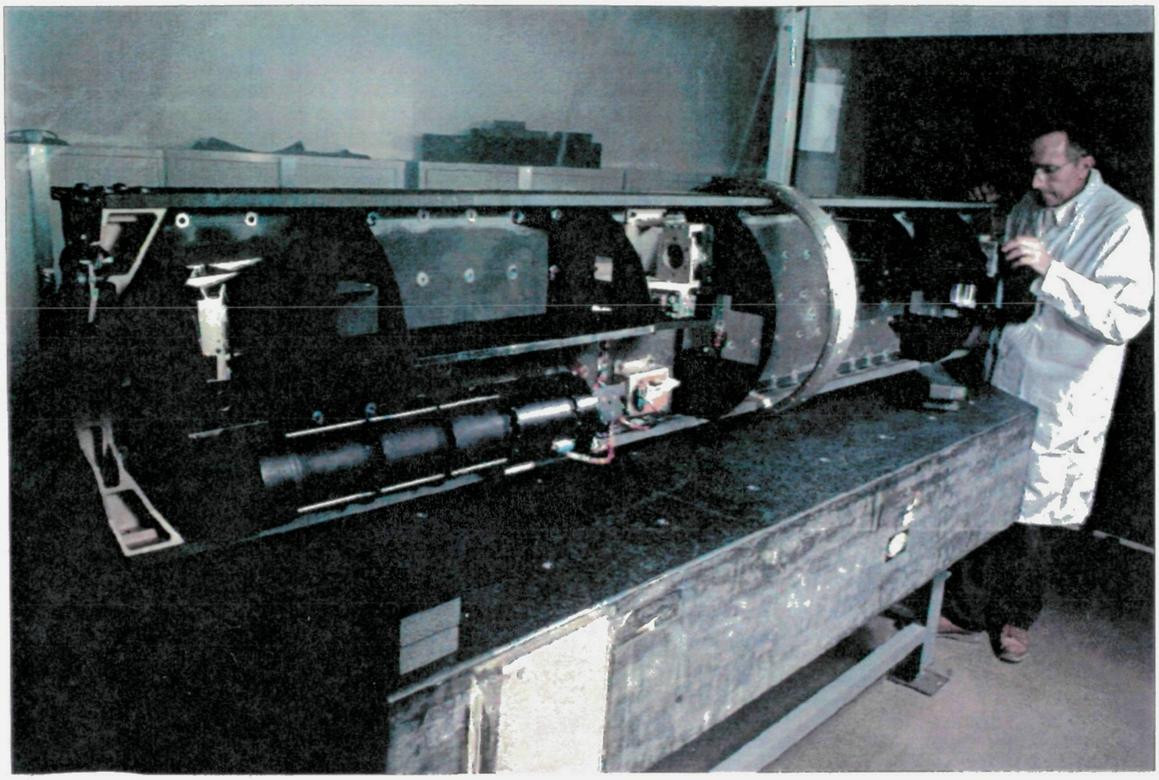

Figure 1: Instrument Scientist Dr. W. A. Brown and the SPDE Payload. The DRSG occupies the top half of the optical table; the UV Imager is seen at the bottom.

2 Payload Preparations

This section will briefly discuss the instrument subsystems that make up the SPDE payload, and indicate the modifications / preparations that have been made under this contract. The SPDE payload, shown in Figure 1 consists of a cluster of optical systems supported by a common optical table structure. The configuration flown on Mission 36.123 included a Dual Range UV / EUV Spectrograph (DRSG), a Normal Incidence X-ray Imager (NIXI), an Ultraviolet Imager (also a normal incidence instrument), and an H-α real-time imaging system. The detector for the Hα imager is a vidicon; its images are used during the mission for in-flight target selection. The other instruments record data on film. A computer-controlled electronic system sequences the operation of the various instruments.

2.1 Dual Range Spectrograph (DRSG)

This is a normal incidence stigmatic system that uses an off-axis paraboloid to form an image of the sun on the entrance slit of a dual toroidal grating spectrograph. One end of the paraboloid is coated for optimum performance in the 1200 to 1400 Å

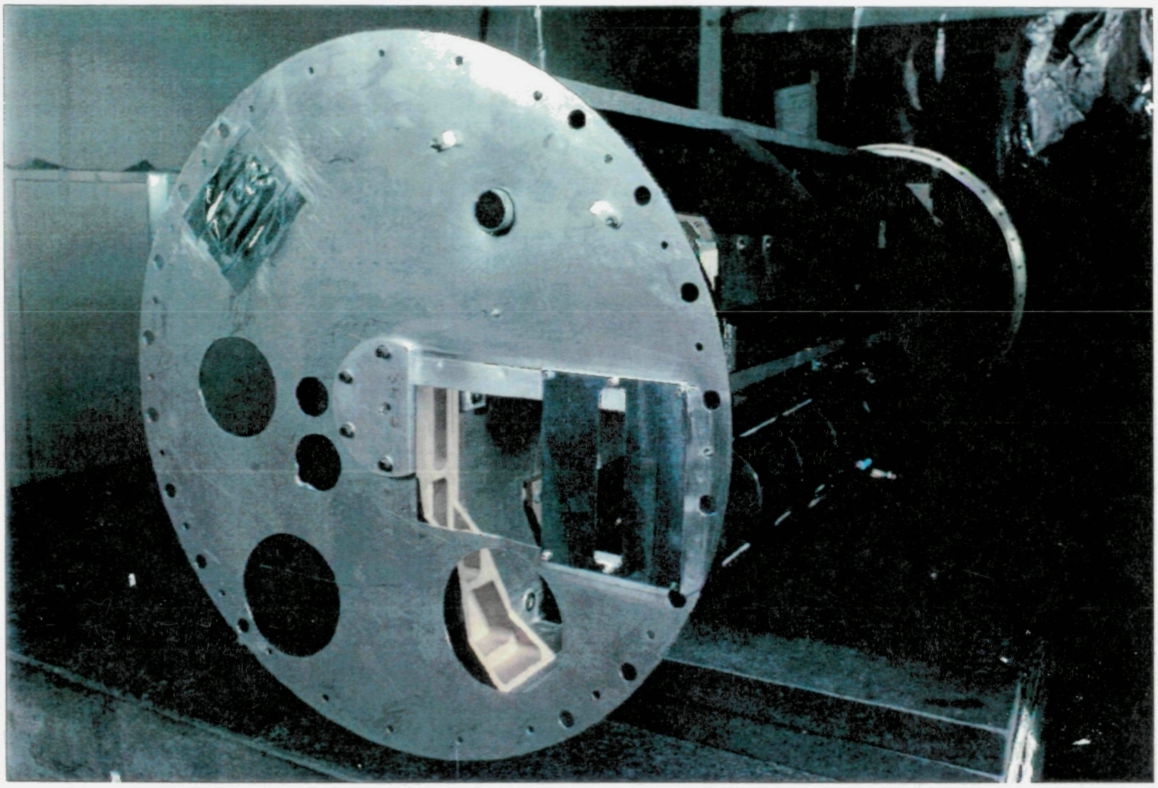

Figure 2: The new DRSG entrance aperture mask is seen on the right side of the aperture plate.

range, and the other end is multi-layer coated for a 40 Å wide band centered around 280 Å. Inside the spectrograph, the two wavelength ranges diverge, striking diffraction gratings designed specifically for each range. The final spectrum image is formed on 35 mm film carried in a Canon T-70 camera back. The spectrographs operate at f/20 and have effective focal lengths of 2 m. Spatial resolution is about 3 arc seconds (Nyquist limited) at the center of the field of view. The spectral resolution is about 7,000 in the EUV and 20,000 in the UV.

The DRSG entrance aperture mask was modified to reduce the collecting area of the UV section so that exposure times are more nearly balanced with the EUV section. The new mask (Figure 2) exposes a 10 cm wide by 2 cm tall area of the UV primary, providing a factor of five decrease in the collecting area. We also decreased the slit width from 25 microns to about 12 microns for a further decrease in the effective collecting area. This change also increased the spectral resolution of both sections of the DRSG. We added a light baffle to the DRSG film transport to improve the isolation between the UV and EUV sections so as to reduce the scattered light level in the latter.

2.1.1 Slit Jaw Camera

The DRSG includes a slit jaw camera for recording the location of the spectrograph slit on the solar disk. The original system consisted of a Canon model T-50 camera body, a lens, aperture stop, and neutral density filters. The slit jaw camera operates in white light. In preparation for the flight of NASA 36.123, we have remounted the lens and camera to eliminate vignetting by the entrance aperture mask, deriving the slit jaw image from the full aperture of the XUV half of the primary mirror. We also increased the aperture of the relay lens and removed most of the neutral density filters in order to improve the spatial resolution of the system. Finally, the Canon model T-50 camera body was replaced by a model T-70 body so that much shorter exposure times could be used. The modified slit jaw camera system has much better imaging properties than the original system.

2.2 Normal Incidence X-ray Imager (NIXI)

The NIXI is a prime focus telescope system in which four spherical objective mirrors are mounted on a turret assembly, seen in Figure 3. Each mirror has a multilayer coating optimized for a different wavelength band in the soft x-ray range. The turret is indexed between exposures in order to change wavelengths. The soft x-ray images are recorded on film carried in a Canon T-70 motorized 35 mm camera back. A thin aluminum filter supported on stainless steel mesh is used to exclude visible light. NIXI was flown on 36.048, but did not record solar images because of a failure of the thin aluminum filter.

We developed and installed a protective shutter system (Figure 4) consisting of a motorized door that covers the camera aperture during launch and recovery and during vacuum operations on the ground. The door is dynamically balanced to reduce any tendency for it to move during vibration testing or launch. A simple electrical interface, limit switches, and appropriate payload harness wiring were added to permit the door to be controlled by the on-board computer.

One new mirror, coated for 63 Å, was prepared and installed. The mirror turret was inspected and found to be in good operating condition. All mirrors were installed and re-aligned, and the instrument focus was re-set.

2.3 H-alpha Imager

This instrument consists of a 3.5 inch diameter Maksutov telescope, a reticule system, a narrow band filter system, and a television camera system. This instrument is fully developed and has been flown in the last five sounding rocket payloads. Its principal function is as an aid to pointing and aspect determination.

In preparation for the 1994 launch, we have refurbished the vidicon detector and re-mounted it, re-established the focus, and re-set the alignment with the DRSG.

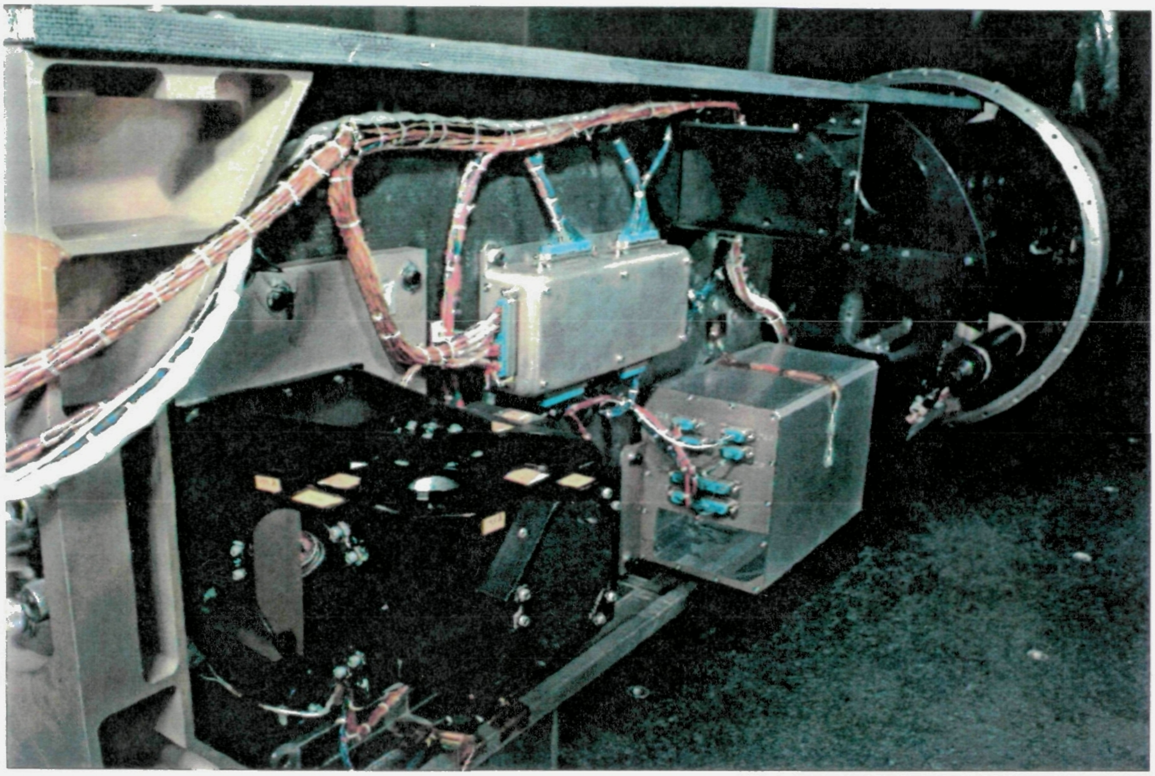

Figure 3: The NIXI turret is seen in the forground, followed by the main junction box and the on-board computer.

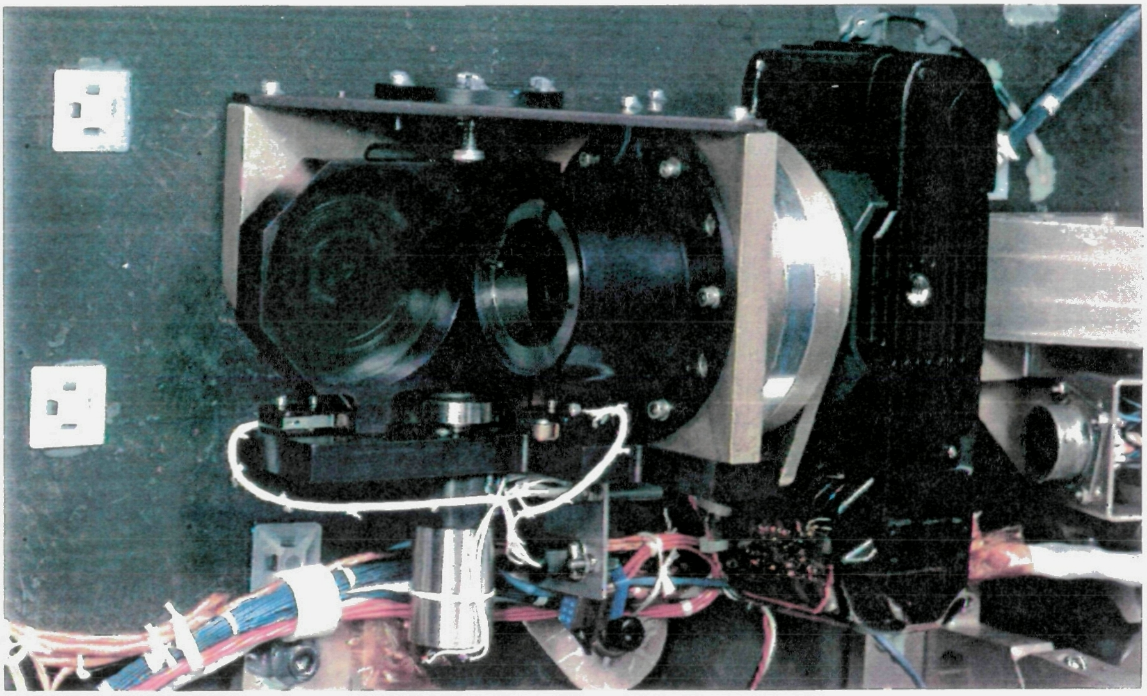

Figure 4: This new motorized door assembly protects the thin aluminum filter of the NIXI film camera during ground operations, launch, and recovery.

2.4 Ultraviolet Imager (UVI)

The UVI has been flown on all previous missions of this program. In past flights, it has been used as an ultraviolet filter camera, making very high spatial resolution photographs at the H-lyman α line and in the continuum near 1600 Å. The wavelength ranges were determined by interference filters placed in front of the focal plane. For the 1994 flight, we procured a new interference filter designed for 1570 Å. It replaced one of the two H Lyman-α filters that were used on the previous flight.

2.5 EUV Imager (EUVI)

The DRSG and UVI systems both require a type of ultraviolet-sensitive photographic film that is no longer being manufactured. Existing stocks of this film are adequate for the forthcoming flight and one or two more, but will eventually be exhausted. The EUVI system is designed as a flight test of a UV sensitive CCD camera system that can eventually replace the film cameras that are now used. It consists of a normal-incidence multilayer mirror herschelian telescope, a mechanical shutter, a thin-film filter (to exclude visible light) the CCD camera, its electronics, and a digital interface / buffer for transferring the data to the telemetry system. Optically, the EUVI is similar to the NIXI; it has a shorter focal length (2 m vs 2.5 m for NIXI) and operates at the single wavelength of 171 Å. The CCD camera head and electronics mounts on the aft end of the optical table, next to the NIXI film transport. The multilayer mirror mounts next to the main junction box, near the NIXI turret. The digital interface / buffer, together with power conditioning modules, fit on the optical table on the forward side of the CCD camera head. The interface / buffer is based on an Ampro PC 104 386SX program card. Software in the microprocessor controls the shutter, initiates CCD integration, commands on-chip summing and read-out of the CCD, captures the digital images, and buffers and formats the data to telemetry. The EUVI system includes a thermo-electric cooler for lowering the temperature of the CCD to about -20 C prior to launch.

Technical difficulties on another program prevented the timely completion of the Lockheed-funded EUVI system, and it could not be fully integrated in time for the 1994 launch. To avoid compromising either the schedule or the technical integrity of the payload, it was decided not to attempt to fly it on NASA 36.123.

2.6 Structural System

The instrument structure is based on a two sided optical table, sized for the 22 inch diameter rocket payload. The table is fitted with a pattern of threaded inserts to allow precision mounting of the optical components of the several telescopes and spectrographs. Thermal stability is assured by the use of carbon-epoxy composite, which has been designed to have a very low coefficient of thermal expansion. A hydrophobic resin system has been used to make the composite, in order to minimize dimensional sensitivity to water content. A support system consisting of end fittings, thrust bearings, and a lateral shear panel carries the launch loads while keeping the optical bench in a strain-free condition following burnout.

The instrument compartment consists of four structural components: two cylindrical sections, an extension ring and the vacuum door. The thrust load is carried by the forward cylinder by means of a spherical bearing assembly that is designed to eliminate torque loads and bending moments on the optical table. This assembly also supplies lateral support to the forward end of the table. The aft end of the optical table is supported laterally and in the roll direction by a shear panel which also contains the instrument apertures. The shear panel attaches to the aft end of the aft cylinder. The two cylinders are separated by an adapter ring that carries a vibration snubber and also serves to support the optical table on a portable work stand whenever the structural cylinders are removed for servicing the instrument. Modified tension joints are used to connect the cylindrical sections to the adapter ring and to the instrumentation compartment at the forward end of the payload. The forward cylinder contains the instrument umbilical connector and a 3 inch vacuum port for evacuating the instrument compartment prior to launch.

The structural system performed nominally during the flight of 36.048. However, the recovery impact caused a collision between the aperture end of the optical table assembly and the vacuum door, damaging the actuator rods on the latter. At our suggestion, an extension ring was manufactured for insertion between the payload compartment and the vacuum door in preparation for the 1994 flight. We also remounted the LISS and MASS sensors and re-arranged internal light baffles so that the payload orientation in the rocket cylinders could be returned to its originally designed position. The damaged vacuum door was refurbished at Wallops Flight Facility.

2.7 Control System

The instrument control system is quite simple, consisting of an on-board microcomputer and appropriate interface circuits. Its primary function is to generate the exposure sequences for the different camera drives. Commands originating in the SPDE Ground Terminal (an Everex 386-20 personal computer) are sent to the onboard computer via an RS232 duplex asynchronous serial communications link. This serial link also returns instrument status information to the SPDE Ground Terminal for display and recording. The baud rate for the serial link is 1200 bits per second. Exposure sequencing and filter settings are controlled either under a program commanded from the ground, or in the event of a communications failure, from a default exposure sequence.

No major modifications to the control system were required, other than the addition of some payload harness wiring to accommodate the new NIXI protective door and the EUVI system. Final programming of the flight E-proms was done in the field, just prior to the flight.

3 Project Initiation Conference

A Project Initiation Conference was held on 14 January, 1994 at the Wallops Flight Facility in preparation for flight 36.123. The flight requirements and mission success criteria are documented in an Experimenters Data Package that was distributed at the meeting. This data package, reproduced in Appendix B of this report, contains a detailed description of the instrument, a new mass budget, and other technical details needed to prepare for the mission.

4 Mission 36.123, Field Activities

4.1 Pre-launch Preparations

The payload and ancillary support equipment were shipped to the White Sands Missile Range in early April, 1995 in preparation for launch. Integration activities were nominal and no serious problems were discovered; a few minor wiring errors were found and corrected. However, the payload rotation in roll, discussed in Section 2.6, above resulted in a substantial and somewhat unexpected change in the dynamic balance of the payload. Compensation for this change required a substantial amount of ballast, increasing the total payload weight. The increased weight forced the reduction of the comprehensive success criterion for time-above-altitude to be decreased from 320 seconds to 300 seconds.

During environmental testing, a vibration-induced alignment alignment shift was discovered in the H-α imaging system. Investigation of the anomaly showed that the retaining ring for the front element of the telescope was loose, allowing the element to shift laterally during vibration. Tightening the retaining ring and staking it with epoxy solved the problem.

The other troublesome aspect of the integration period centered around the new SPARCS command console, which replaced the ASCL system used for all of our previous flights. Mission 36.123 represented the first use of the new system for solar observations. New flight-specific software was still being developed during the launch preparations, and the final version was not ready in time for adequate practice by the experiment team. The new display system suffered from a lack of brightness and contrast in comparison to the ASCL monitors that were previously used. Moreover, adjustments to contrast and brightness had to be made by opening windows on the display and moving on-screen "sliders" with a mouse. The older system in which one simply rotated a knob on the panel was much more intuitive, and is superior in our opinion. Finally, the computer link between the SPARCS command console and the SPDE ground terminal could not be made to work, forcing those operations to be done manually. In retrospect, we believe that the manual mode is simpler and probably preferable for this type of mission.

In spite of these minor difficulties, the integration and final flight preparations went very smoothly, thanks to the high degree of professionalism exhibited by the WSMR launch team. The preparations were completed on an abbreviated schedule by virtue of the hard work put in by these dedicated people. NASA is indeed fortunate to have them.

4.2 Observing Campaign

In order to maximize its scientific value, Mission 36.123 was carried out as part of a coordinated observing campaign with the Yohkoh Soft X-ray Telescope (SXT) and several ground-based observatories. Cooperating ground-based observatories included the Owens Valley Radio Observatory (OVRO), The National Optical Astronomy Observatory at Kitt Peak, and the Mees Solar Observatory. The Big Bear Solar Observatory could not observe because of cloudy weather. The NOAA Space Disturbance Forecast Center in Boulder, Colorado assisted with predictions and communications. The Yohkoh observations were particularly helpful, as they provided current images of the sun in soft x-rays about two hours before the scheduled launch time. Final target selection was based on these images, and the coordinates were relayed to the ground-based observers via the NOAA facilities.

The dataset from these sources includes simultaneous soft x-ray images from Yohkoh, radio images from OVRO, magnetograms and He I λ 10830 spectroheliograms from Kitt Peak, and H α images, H α stigmatic spectra, and vector magnetograms from Mees.

4.3 Rocket Flight

Mission 36.123 was launched on schedule at 20:45 UT on 25 April. The launch was perfect, and the attitude control system performed well. Minor problems with the SPARCS command link delayed the start of science exposures, but they were finally initiated at about T+140 seconds. Most of the DRSG exposures were made on NOAA active region 7704; toward the end of the flight, a few were taken of AR 7705. On at least two occasions, the on-board computer hung, apparently due either to some sort of electrical interference or to non-standard command sequences that were used to accommodate the delayed start of observations. The computer was re-started each time by ground command. Observations were terminated at T+403 seconds by the loss of fine pointing and subsequent closing of the vacuum door.

Payload recovery was nominal, and a crushable section that was added to the vacuum door absorbed most of the impact. Substantial surface winds in the recovery caused the payload to be dragged through the desert for several hundred feet before the parachute was collapsed by a member of the recovery team. There was no damage to the payload hardware. In particular, the new protective door for the thin aluminum filter in the NIXI system performed well, and the filter was recovered in perfect condition. The payload was still under vacuum when returned to the laboratory.

Development of the flight film revealed a wealth of new data: Two excellent image sequences were obtained in Fe IX and Fe XI with the NIXI. The ultraviolet imaging system recorded excellent images in the hydrogen Lyman-α line and one usable exposure in the C IV line. The re-designed mask and stray baffle system for the DRSG was successful in balancing the exposure levels between the UV and EUV sections. The modified slit jaw camera system worked as designed, producing well exposed images suitable for aspect determination.

The initial inspection of the flight results showed that both the Minimum and the comprehensive success criteria that were established for 36.123 had been exceeded. A summary report on the project, discussing the success criteria and detailing our experience with the new Sparcs Command System, was sent to Mr. Larry Early of Wallops Flight Facility (Code 840) at his request. A copy of the letter is included as Appendix C of this report.

5 Data Reduction and Archiving

Densitometry of the flight films was carried out at the Lockheed-Martin Palo Alto Research Labs, using a CCD based digital microdensitometer system. Because of the finite array size of the CCD, only a limited area on the film could be digitized at one time, if the full resolving power of the film was to be maintained. Alternatively, we could sacrifice spatial resolution in favor of a larger area coverage on the film. Both approaches were used, the latter for co-alignment of the images and line identification of the spectra; the former for detailed study of active region loops and other features of the images or to retain the full spatial and spectral resolution of the stigmatic spectra. Since there are several different exposures in each sequence taken from each instrument, the densitometry effort was prolific in its creation of files. There are about 150 files in all, totaling around 600 megabytes for the raw database.

Much of the densitometry and line identification effort was performed by Dr. W. A. Brown, who was available to us as a small business subcontractor. Dr. Brown served as the SPDE instrument scientist prior to his retirement in 1994. As a subcontractor, Dr. Brown's services were secured on very favorable terms, allowing us to accomplish a great deal more than would have otherwise been possible. Dr. Brown's contract reports are reproduced as Appendix D of this report.

In order to enhance the availability of the data, we have prepared a digital archive containing all of the densitometer data from the 1992 and 1994 flights, as well as a subset of the densitometry for which conversions to intensity have been made.

It must be stressed that the intensity values are based on relatively old published values for the film sensitivity, and may contain substantial errors. Available funding has not permitted us to do new sensitometry of the flight film, though enough of it remains to do new calibration work if the opportunity presents itself. At this time, the data files together with relevant utility software and some co-aligned image sets reside in an on-line directory in the Lockheed Solar & Astrophysics computer network in Palo Alto; they are available to Yohkoh investigators and other interested parties. We have also prepared a CD ROM containing the entire database, a copy of which is submitted with this report. The structure of the directory tree and further details of the database are given in Appendix E. A description of the SPDE program and samples of flight data have been placed on the World Wide Web at (http://www.space.lockheed.com/SPDE/welcome.html).

6 Preliminary Results from Mission 36.123

Initial analysis of the flight data began with the preparation of a co-aligned image set containing the NIXI, UV, Yohkoh, and ground-based data. We then used a computer workstation to perform blink comparisons between images formed at different temperatures or between filtergrams and magnetograms. This section will describe some of our first results.

6.1 Active Region Loops

A number of loop systems were seen in the two modest active regions that were visible on 25 April. The appearances of the loops seen in Fe IX and 171 Å and in Fe XII at 195 Å are qualitatively very similar. However, substantial differences are found between these images and those recorded simultaneously by the SXT. Figure 5 shows a co-aligned pair of images that illustrate this point. Figure 5 (a) was made by SXT with the thin aluminum filter, which responds principally to temperatures in the 2–5 million K range. Figure 5 (B) shows the same region in the NIXI Fe IX image, which is most sensitive to temperatures in the 0.8–1 million K range. Both images are shown as negatives. It is readily apparent that their morphologies are quite different. To aid in the comparison, isophotes have been added to two relatively isolated loops in the SXT image and their locations shown on the Fe IX image. In both cases, the Fe IX emission is weakest near the center of the SXT loops, and the latter's presence would not be inferred from the Fe IX images alone. However, we note that bright Fe IX emission is found near the ends of both SXT loops; one cannot rule out the possibility that they are physically connected.

When a blink comparison is done between the SXT and either of the NIXI images, one gets the impression that two types of structures are present, one representing the locus of the footpoints of the hotter SXT loops and the other consisting

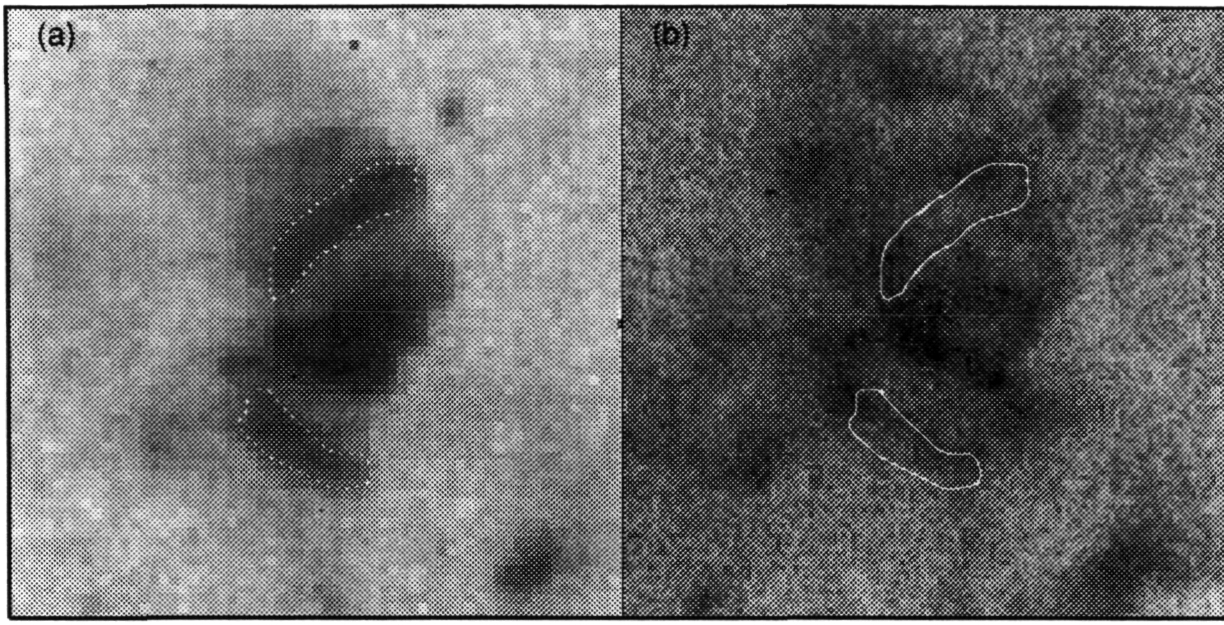

Figure 5: Co-aligned soft X-ray images of an active region, recorded during flight 36.123. Panel (a) is from the Yohkoh SXT; panel (b) is the NIXI 171 Å image. Isophotes from two relatively isolated loops in the SXT image demonstrate the differences in morphology between the hot and cooler coronal plasma.

of spatially isolated, cooler loops that are visible in their entirety in Fe IX. We also reached this conclusion from our comparison of the 1992 C IV images with structures seen simultaneously in SXT. However, we found the transition region footpoints to be more compact than is the case for the Fe IX images. This is consistent with the larger scale heights expected for the hotter plasma that is visible in Fe IX. These findings were presented in a paper given at the 1994 COSPAR meeting in Hamburg, Germany.

The quantitative active region data, including the spectra, are being studied by Mr. Brian Handy of the Montana State University as the subject of his doctoral dissertation. Mr Handy is in residence at Lockheed, though he receives his support from Montana State University. Handy's thesis director is Dr. Loren Acton, who has been involved for many years with the SPDE program and its predecessors.

6.2 Coronal Bright Points

The 1994 NIXI data also provide an excellent opportunity for the study of coronal bright points; many are visible in both the Fe IX and Fe XII images. In comparing them with co-aligned images made with the SXT, we find that there is a one-to-one correspondence between bright points seen in the NIXI images and those observed by SXT. However, they are much more prominent in the NIXI images. Many bright points that are easily seen in Fe IX and Fe XII are barely recognizable in the SXT data. Our interpretation is that these structures are relatively cool with most of their emission measure arising from temperatures lower than 2 million K. These observations quite effectively answer the question of why coronal bright points have been difficult to see in the SXT images.

6.3 Coronal Holes

The sensitivity of the Fe IX and Fe XII images to relatively cool coronal material makes them useful for the unambiguous identification of coronal holes. In Figure 6, we present a set of simultaneous full-disk images from the 25 April campaign. The arrow on the figure identifies a coronal hole that is visible in both EUV channels, the SXT image and in a He 10830 Åimage taken at Kitt Peak. Note, however, that in the SXT image, the hole appears to extend northward to and beyond the north limb. Relying on SXT alone, we would be tempted to identify this northern extention as part of the coronal hole. The Fe IX and XII show that this is not the case; both show the presence of cool coronal material in the "northern extension". A similar region is seen in the Southwest quadrant of the disk. These findings have important implications for the determination of coronal hole temperatures from SXT data, such as those recently reported by Hara, et al. (1994). In the absence of the low temperature data, coronal holes could easily be mis-identified.

7 Summary

The SPDE investigation has succeeded in both its scientific and its technological aspects. Flight 36.123 was successful in producing a wealth of new data, suitable for a variety of investigations, well beyond the scope of this program. The images from the NIXI instrument have proved to be especially interesting. Several presentations and papers incorporating the data have been produced. A permanent data archive has been created in CD ROM format to preserve the database for future investigations by other interested scientists. The two successful flights of the rocket payload have convincingly demonstrated the utility of our re-configurable payload concept for low-cost missions. Finally, a set of World Wide Web pages have been created to make the instrument details and a subset of the flight data immediately available to the scientific community.

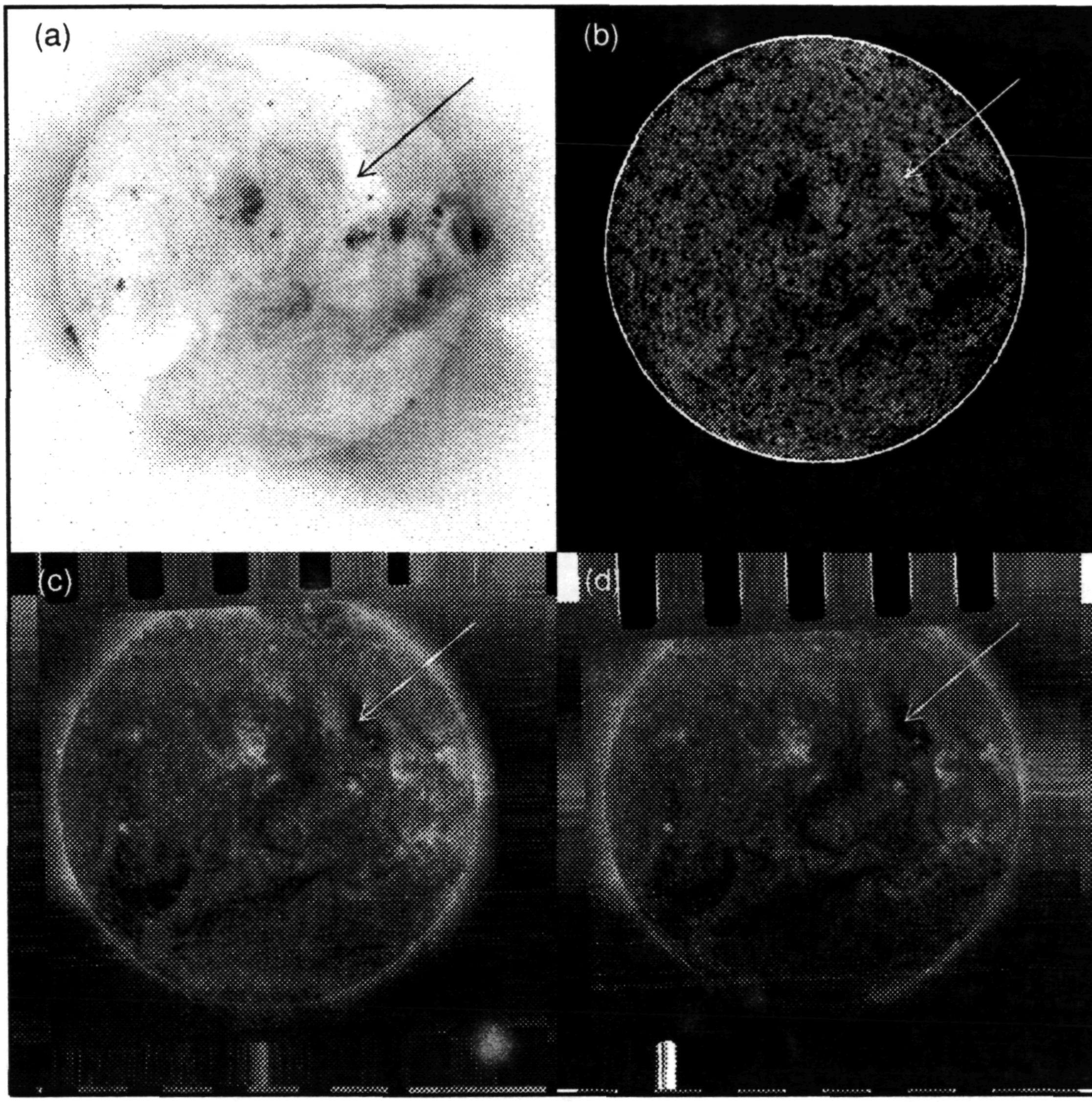

Figure 6: Full disk images from the 1994 25 April campaign. Panel (a) (shown as a negative image) was made by the SXT on Yohkoh. Panel (b) is the He II 10830 Å image from Kitt Peak. Panels (c) and (d) are the NIXI Fe XII and Fe IX images, respectively. The arrows show the location of the coronal hole discussed in the text.

A Publications and Presentations

This section presents a list of presentations and papers that have resulted from this investigation. Also included in the list are several publications that were prepared under prior contracts of this investigation (NAS5-2-9181, NAS5-25727 and HAS5-29739) but were inadvertently omitted from the respective final reports. Entries dated 1992 and earlier are in this category.

Damé, L., Martić, M., Brown, W.A., Bruner, M.E., Strong, K., Suematsu, Y. Tsuneta, S. and Schmieder, B.: Coordinated SPDE Rocket, YOHKOH and Ground Observations of an Emerging Flux Region and a Filament, Adv. Space Research, 17(4/5), 189-192, 1996

Strong, K.T. and Bruner, M.E.: A New Perspective On Solar Active Regions, Adv. Space Research, 17(4/5), 179-188, 1996

Bruner, M.E., Brown, W.A., Lemen, J.R., Morrison, M. Strong, K.T., and Hirayama, T.: The Corona–Transition Zone Interface, Presented at the 30th COSPAR Scientific Assembly, Hamburg Germany, 11-21 July, 1994.

Brown, W.A., Bruner, M.E.: UV and EUV Line Ratios from SPDE Solar Rocket Observations. Presented at the 1994 Spring meeting of the AGU.

Foing, B.H., Wiik, J.E., Martens, P. and Fleck, B.: Transition Region Camera Results on Flares and Eruptive Prominences, Presented at the 30th COSPAR Scientific Assembly, Hamburg Germany, 11-21 July, 1994.

Shing, L., and Catura, R.C.: Time Stability of Multi-layer Reflectivity, Proc. SPIE 2279, 204-210, 1994.

Brown, W.A., Bruner, M.E. and Dame, L.: Observation of Density Sensitive Lines in the Solar UV Spectrum. Presented at the Dec., 1993 AGU meeting, San Francisco, CA.

Damé, L. and Guyenne, T.D. (Eds.): Proceedings of the ESA Workshop "Solar Physics and Astrophysics at Interferometric Resolution", Paris, 17–19 February 1992, ESA SP–344, ISBN 92-9092-218-4, May 1992 (322 pages)

Foing, B., Damé, L. and Martić, M.: Rocket Observations and Modelling of Flux Tubes, Advances in Space Research, 11(5), 245 (1991)

Martić, M., Damé, L., Bruner, M.E. and Foing, B.: TRC 4: Correlation of the Tmin fine structure with the chromospheric bright points, Advances in Space Research, 11(5), 241 (1991)

Damé, L., Heyvaerts, J. and Foing, B.: Possible Scenarios of Coronal Loops Reconnection/Heating Processes to be Observed at High Spatial Resolution, Advances in Space Research, 11, 327 (1991)

Shing, L. and Cature, R.C., Fabrication and Analysis of Mo-Si Multilayers, Proc. SPIE 1546, 607-613, (1991).

Martić, M. and Damé, L.: High Resolution Diagnostic of the Mesocells in the Solar Temperature Minimum Region, in Solar and Stellar Granulation, Eds. R.J. Rutten and G. Severino, Kluwer Academic Publishers, 207-215 (1989)

Martić, M. and Damé, L.: Rocket Flight Observations of the Meso-Scale Structure in the Temperature Minimum Region, Advances for Space Research, 8(7), 173 (1988)

Foing, B., Martić, M., Bonnet, R.M., Damé, L. and Bruner, M.E.: Advances for Space Research, 8(7), 221 (1988)

Damé, L., Foing, B., Martić, M., Bruner, M.E., Brown, W.A., Decaudin, M. and Bonnet, R.M.: New Ultra-Violet Filtergrams and Results from the Transition Region Camera Rocket Experiment, Advances for Space Research, 6(8), 273 (1986)

B Experimenter's Data Package

Solar Plasma Diagnostics Experiment (SPDE)

Project Initiation Conference
14 January, 1994

Experimenter's Data Package

Dr. M. E. Bruner, Principal Investigator
Lockheed Palo Alto Research Laboratory
Contract NAS5-32147

Contents

Solar Plasma Diagnostics Experiment (SPDE)

Project Initiation Conference

Experimenter's Data Package

Dr. M. E. Bruner, Principal Investigator
Lockheed Palo Alto Research Laboratory
Contract NAS5-32147

1 OVERVIEW

1.1 Scope

This document will present technical information on the Solar Plasma Diagnostics Experiment payload. The scientific objectives were described in detail in Lockheed proposal number LMSC-D088449, dated 2 July, 1984, and will be treated only very briefly here. The hardware was developed under previous contracts, and was flown on NASA Mission 36.048. Modifications have been incorporated into the payload to improve performance and to correct problems that arose during mission 36.048. One new instrument subsystem is being added to the payload; a CCD-based soft x-ray imaging system. We would like to fly the payload during April, 1994.

1.2 Objectives

The objective of this investigation is the study of the physics of the solar corona and the underlying chromosphere using the techniques of high resolution imagery and spectroscopy in the ultraviolet and soft x-ray regions of the spectrum. The thrust of the investigation is twofold. First is an exploratory phase in which we study the sun with new, state of the art instrumentation, to see what discoveries may be made when we open our eyes in new ways. In the second phase we seek to interpret the data in terms of physical processes and conditions in the regions that we observe. The emphasis in the first phase is on high resolution spectroscopy and imaging in soft x-rays and in the ultraviolet.

Our primary tool in the second phase of the investigation is diagnostic spectroscopy applied to the soft x-ray and UV spectra, guided by analysis of the soft x-ray and UV images which give both geometric and radiometric boundary conditions. The essence of the analysis is straightforward. From the intensities of allowed transitions, we derive the emission measure, defined as the integral of the square of the electron density over the emitting volume. There are also a number of lines that are density sensitive in the sense that their intensities are not directly proportional to the emission measure, but have some other dependence. Line ratios among lines of differing density dependence are used to infer the electron density of the emitting region. Both the emission measure and the electron density are determined as functions of temperature by selecting appropriate ions. By combining the emission measure found in each temperature interval with the electron density determined for the same intervals we can derive the volume of the plasma that lies within each interval. This, together with the geometry, forms a fairly complete physical description of the plasma that can be compared with theoretical predictions.

1.3 Program History & Status

This program is an outgrowth of our high resolution solar studies work, which began in 1976. The instrumentation developed under the program included a high resolution x-ray Spectrograph-Spectrometer Telescope (XSST), a high resolution UV imaging system (prepared in France under Dr. R. M. Bonnet), an H–α imaging system, a normal incidence soft x-ray imaging system, and a dual-range UV / EUV spectrograph. The current version of the payload includes the following elements:

- The Dual Range UV–EUV Stigmatic Spectrograph (DRSG).

- The Normal Incidence Soft X-ray Imager (NIXI) based on multilayer mirror technology.
- The Ultraviolet Imager (UVI).
- The H-alpha imaging system (H-α).
- A new normal incidence EUV Imager (EUVI) using a multilayer and an EUV sensitized CCD camera.
- A versatile structural system based on an optical table in a 22 inch diameter evacuated cylinder.
- A computer based electronic control system, including a full duplex RS-232 control link and ground terminal for real-time control of the experiments.

Accomodations are included for a stigmatic Flat Field Spectrograph (FFSG) that is planned for future investigations. The DRSG, NIXI and UVI record images on film; the H-α system uses a vidicon detector. More complete descriptions of the instrument are given in the next section and in Appendix A.

2 INSTRUMENT HARDWARE

2.1 Dual Range Spectrograph (DRSG)

This is a normal incidence stigmatic system that uses an off axis paraboloid to form an image of the sun on the entrance slit of a dual toroidal grating spectrograph. One end of the paraboloid is coated for optimum performance in the 1200 to 1400 Å range, and the other end is multi-layer coated for a 40 Å wide band centered around 280 Å. Inside the spectrograph, the two wavelength ranges diverge, striking diffraction gratings designed specifically for each range. The final spectrum image is formed on 35 mm film carried in a Canon T-70 camera back. The spectrographs operate at f/20 and have effective focal lengths of 2 m. Spatial resolution is about 3 arc seconds (nuquist limited) at the center of the field of view. The spectral resolution is about 7,000 in the EUV and 20,000 in the UV. The DRSG was included in the 36.048 payload.

2.1.1 Slit Jaw Camera

The DRSG includes a slit jaw camera for recording the location of the spectrograph slit on the solar disk. This system consists of a Canon model T-50 camera body, a lens, aperture stop, and neutral density filters. The slit jaw camera operated in white light for the previous flight. We are currently investigation the feasibility of adding a narrow band filter centered on H-α for the forthcoming flight. This filter, if included will have a neglegible impact on the weight or the mechanical and electrical propertics of the payload.

2.2 Normal Incidence X-ray Imager (NIXI)

The NIXI is a prime focus telescope system in which four spherical objective mirrors are mounted on a turret assembly. Each mirror has a multi-layer coating optimized for a different wavelength band in the soft x-ray range. The turret is indexed between exposures in order to change wavelengths. The soft x-ray images are recorded on film carried in a motorized 35 mm camera back. A thin aluminum filter supported on stainless steel mesh is used to exclude visible light. NIXI was flown on 36.048, but did not record solar images because of a failure of the thin aluminum filter. A protective shutter system has been developed for the NIXI for the forthcoming flight.

2.3 H-alpha Imager

This instrument consists of a 3.5 inch diameter Maksutov telescope, a reticule system, a narrow band filter system, and a television camera system. This instrument is fully developed and has been flown in the last five sounding rocket payloads. Its principal function is as an aid to pointing and aspect determination. The vidicon detector was refurbished following the flight of 36.048

2.4 Ultraviolet Imager (UVI)

The UVI has been flown on all previous missions of this program. In past flights, it has been used as an ultraviolet filter camera, making very high spatial resolution photographs at the H-lyman α line and in the continuum near 1600 Å. The wavelength ranges were determined by interference filters placed in front of the focal plane. For the forthcoming flight, we are preparing a new set of filters that will permit us to determine the emission measure in the chromosphere and transition regions and the effective temperature of the temperature minimum region, as well as recording the geometry of the magnetic field as revealed by the H Lyman-α line.

2.5 EUV Imager (EUVI)

The DRSG and UVI systems both require a type of ultraviolet-sensitive photographic film that is no longer being manufactured. Existing stocks of this film are adequate for the forthcoming flight and one or two more, but will eventually be exhausted. The EUVI system is designed as a flight test of a UV sensitive CCD camera system that can eventually replace the film cameras that are now used. It consists of a normal-incidence multilayer mirror herschelian telescope, a mechanical shutter, a thin-film filter (to exclude visible light) the CCD camera, its electronics, and a digital interface / buffer for transferring the data to the telemetry system. Optically, the EUVI is similar to the NIXI; it has a shorter focal length (2 m vs 2.5 m for NIXI) and operates at the single wavelength of 171 Å. The CCD camera head and electronics are mounted on the aft end of the optical table, next to the NIXI film transport. The multilayer mirror is mounted next to the main junction box, near the NIXI turret. The digital interface / buffer, together with power conditioning modules, are mounted on the optical table on the forward side of the CCD camera head. The interface / buffer is based on an Ampro PC 104 386SX program card. Software in the microprocessor will control the shutter, initiate CCD integration, command on-chip summing and readout of the CCD, capture the digital images, and buffer and format the data to telemetry. A data package on the EUVI subsystem is given in Appendix **??**. The EUVI system includes a thermo-electric cooler for lowering the temperature of the CCD to about -20 C prior to launch.

2.6 Structural System

The instrument structure is based on a two sided optical table, sized for the 22 inch diameter rocket payload. The table is fitted with a pattern of threaded inserts to allow precision mounting of the optical components of the several telescopes and spectrographs. Thermal stability is assured by the use of carbon-epoxy composite, which has been designed to have a very low coefficient of thermal expansion. A hydrophobic resin system has been used to make the composite, in order to minimize dimensional sensitivity to water content. A support system consisting of end fittings, thrust bearings, and a lateral shear panel carries the launch loads while keeping the optical bench in a strain-free condition following burnout.

The instrument compartment consists of four structural components: two cylindrical sections, an extension ring and the vacuum door. The thrust load is carried by the forward cylinder by means of a spherical bearing assembly that is designed to eliminate torque loads and bending moments on the optical table. This assembly also supplies lateral support to the forward end of the table. The aft end of the optical table is supported laterally and in the roll direction by a shear panel which also contains the instrument apertures. The shear panel attaches to the aft end of the aft cylinder. The two cylinders are separated by an adapter ring that carries a vibration snubber and also serves to support the optical table on a portable work stand whenever the structural cylinders are removed for servicing the instrument. Modified tension joints are used to connect the cylindrical sections to the adapter ring and to the instrumentation compartment at the forward end of the payload. The forward cylinder contains the instrument umbilical connector and a 3 inch vacuum port for evacuating the instrument compartment prior to launch. A complete set of mechanical drawings was delivered as part of the Design Review Package for mission NASA 36.048. The structural system performed nominally during the flight. However, the recovery impact caused a collision between the aperture end of the optical table assembly and the vacuum door, damaging the actuator rods on the latter. We suggest that an extension ring be inserted between the payload compartment and the vacuum door prior to the forthcoming flight. The mass of this extension ring should be compensated by reducing the amount of ballast carried within the payload compartment, maintaining the payload weight & balance.

2.7 Control System

The instrument control system is quite simple, consisting of an on-board microcomputer and appropriate interface circuits. Its primary function is to generate the exposure sequences for the different camera drives. Commands originating in the SPDE Ground Terminal (an Everex 386-20 personal computer) are sent to the on-board computer via an RS232 duplex asynchronous serial communications link. This serial link also returns instrument status information to the SPDE Ground Terminal for display and recording. The baud rate for the serial link is 1200 bits per second. The control system is described in more detail in Appendix A. A set of electronic schematic drawings was provided as part of the Design Review Package for NASA 36.048. The new EUVI system will require about 0.75 A at 28 V for preconditioning / cooling the CCD prior to launch. The payload's on-board control computer will need to be operated during this interval in order to monitor the CCD temperature as well as the status of the other payload subsytems.

2.8 Redundant Systems

2.8.1 Shutter and Motion Commands

Shutter and motion system commands are redundantly provided by the microcomputer system, under normal conditions, or thru discrete AUX SW commands.

2.8.2 Sequencing

Exposure sequencing and filter settings are controlled either under a program commanded from the ground, or in the event of a communications failure, from a default exposure sequence.

2.8.3 Microcomputer Watchdog Timer, Power-fail

The microcomputer has a watchdog timer which will reset the processor in the event of some upset. In addition, a band-gap power fail detection unit monitors the supply voltage and signals the processor in the event of a power failure. The processor may also be reset by use of an AUX SW command.

2.8.4 Redundant Message Transmission

When a message is received via the serial link, it is verified. In the event of a failure, the message is transmitted again.

2.9 Payload Weight Changes

The modifications and additions discussed earlier in this section will have a minor impact on the total payload weight. Most of the added weight is near the aperture (aft) end of the payload so that it improves the payload balance. We request that to the greatest extent possible, the added weight in instrument hardware and the requested new extension ring be compensated by removing internal ballast, minimizing the total payload weight. Table 1 summarizes the added payload weights and their locations. The station locations given in the following table are referred to the nose tip of the rocket,

Table 1

Item	Mass	Station
NIXI Door Assembly	0.28	5.65
EUVI Mirror Assembly	1.32	3.60
CCD Camera System	5.89	5.70
Baffle	0.50	4.90
CCD Interface / Buffer	$\simeq$1.5	$\simeq$5.4
CCD wiring Harness	$\simeq$0.7	$\simeq$4.0
Total	$\simeq$9.5	

Table 1: Masses and locations of added equipment. Masses are in kg, station locations are in m and are referred to the rocket nose tip. Harness weight includes a 0.2 kg allowance for fasteners and misc. hardware.

as shown in Figure 5a of the Flight Requirements Plan for Terrier-Black Brant VC 36.048, signed by L. J. Early on 22 January, 1992. Masses are given in kg; stations in m. Masses of added components are measured when available, otherwise are calculated from CADAM drawings of the individual parts. The mass of the CCD interface / buffer is not yet known; it is estimated to be about 1.5 kg at station 5.4 m.

To these weights, must be added the weight of the requested extension ring, which begins at station 6.03.

3 ROCKET SUPPORT SYSTEMS REQUESTED

3.1 General Requirements

The science instrument payload is aft looking. It is designed to fit within a 22 inch o.d. by about 122 inch long structural cylinder, and to be launched on a Terrier boosted Black Brant V rocket. A bulbous payload configuration is assumed, as was used on NASA 36.048. It has tapered transition sections containing the flight instrumentation on the forward end of the instrument compartment and the igniter housing and separation assembly on the aft end. The structural cylinders, rings, and bulkheads were successsfully recovered following 36.048, and are suitable for re-use, pending the completion of normal pre-flight environmental testing.

3.2 Vacuum

The instrument compartment is to be evacuated, and a "toilet seat" style vacuum door is required between the aft end of the instrument and the rocket separation assembly. It is assumed that the structural components of the rocket (cylinders, adapter rings, vacuum doors, etc.) are government furnished; presumably they will be the existing units. Use of the SPARCS turbomolecular pumping station on the launch pad is requested. A supply of clean, dry nitrogen for backfilling the payload is also requested, as is an improved procedure to avoid problems with dust in the payload.

Vacuum connection to the payload will be via a 3 inch port. As stated earlier, the vacuum door assembly was damaged during the recovery of the 36.048 payload, and needs to be refurbished. We recommend that a crushable shock absorber be installed on the exterior (aft) surface of the door for the forthcoming flight to cushion the payload against the recovery impact.

3.3 SPARCS, ASCL & S-19 Systems

A SPARCS control system and use of the Automatic Sparcs Control Link (ASCL) (or its equivalent) are requested. Use of LISS and MASS solar attitude sensors is assumed. Use of the S-19 stabilization system during launch is also requested, and a rail launch is assumed. We also request that a parallel link between the SPDE Ground Support Console and the ASCL computer be provided (as on 36.048) for use in synchronizing the ASCL pointing program with the payload observing sequence.

3.4 RS-232 Command Link, Telemetry & Power

An RS-232 duplex communications link is requested for instrument command and a TV downlink is needed for ASCL use. Limited telemetry is needed for housekeeping purposes. A 1.6 mbps digital telemetry link is requested for the CCD camera data. Experiment power is expected to be in the range 5 to 9 amperes @ 28 volts.

3.5 Observing Time, Pointing Stability, Recovery

A minimum of 250 seconds (with a goal 300 seconds) of observing time above 80 km is required to meet the science objectives *excluding the time for acquisition of the sun by SPARCS.* Pointing stability should be of the order of $\pm 1 arcsec$ or better. Parachute recovery of the payload is required. The parachute used for flight 36.048 appeared to be near the limit of its capacity, and resulted in a fairly hard landing. We request that serious consideration be given to use of a parachute recovery system with a higher load capacity.

3.6 Other Support Requirements

3.6.1 LPARL Microcomputers

LPARL provided GSE will include two PC-class computers. At launch one will be located at the control center and one in the blockhouse.

The blockhouse PC will be connected to the umbilical from the experiment and will be used for vertical checkout. The connection to the umbilical and 115 volt, 60 Hz. power are the only requirements for the block house computer.

The control room computer (the SPDE Terminal Computer) will be used to run the experiment via the serial link. The control room computer will also be used to signal the ASCL when to proceed to the next step of the science data scan. The control room computer therefore needs the connections to the serial command and data link to the experiment and the connection to the ASCL port provided for this purpose. Modifications to the ASCL software to accommodate this requirement were made and successfully used during the flight of 36.048. Access to a phone line for modem link from the control room to outside or to the block house is desirable but not necessary nor required.

Data from the Soft X-ray Telescope (SXT) on the Japanese Yohkoh spacecraft will be used for target selection prior to the forthcoming launch, as was done for 36.048. These data are available from Japan via Ethernet. Ethernet support during the entire period of the field activities is requested to accommodate this requirement, preferrably in building N-200.

3.6.2 Strip Charts

Visibility of bilevel data in real time during the flight and recording for post-flight analysis is necessary as a contingency should the main experiment status pathway fail. Strip charts of the status bilevels, one bit per pen, would be the most desirable way of accomplishing this. Strip chart recordings and real-time visibility of the five voltage monitor channels are also a requirement.

3.6.3 Discrete Commands

The instrument shutters and motion mechanisms have, as a back-up to the normal microprocessor commanding, a separate path thru the discrete commands. We should be prepared to issue these commands in the event of experiment microcomputer system failure.

4 FLIGHT PLANS

4.1 Overview

The major objective of the forthcoming flight is the extension of our study of active regions, and coronal bright points, in collaboration with the Yohkoh SXT. We intend to enlist the aid of ground based observers as in the past, to supplement the flight measurements. The flight will be coordinated with observations from the VLA if available, and with one or more ground-based optical observatories. The scheduling of our prime launch window will depend on which observatory is designated as prime. If the Canary Island or Tenerife observatories are prime, then the launch window will be early in the morning. If Hawaii is prime, then the launch window will be later in the day; probably near or shortly after local noon at WSMR. Timing within these broad ranges must be such that the Yohkoh spacecraft is in a phase of its orbit for daylight observations free of the South Atlantic Anomaly (SAA). An ephemeris of Yohkoh will be available within two or three weeks of the selected launch date for planning purposes.

Use of the ASCL Tracking mirror during the pre-launch preparations is requested to test the ASCL and flight software, and for simulated flight operations.

4.2 Experiment Related Events

Experiment related events for the flight will be similar to those for Mission 36.048. The payload will be launched under vacuum. Following SPARCS enable and acquisition of the sun, a Pitch-Yaw sequence will be executed to bring the target area near to the center of the field of view of the H-α system. The major data taking will be done using a three-position linear scan sequence, as was done on 36.048. The same ASCL software that was used for 36.048 will be applicable, if ASCL is used for this mission. If a newer interactive pointing system is used instead, equivalent software will need to be prepared by the SPARCS project team. At the conclusion of the data taking portion of the flight, the vacuum door should be re-closed prior to predicted re-entry, or upon loss of SPARCS fine pointing as has been done on our past flights.

4.3 Pointing Requirements

The instruments must be pointed to selected targets on the solar disk in order to make the required observations. Pointing stability should be $\pm 1 arcsec$ or better, once the desired location has been acquired. There is no special requirement for absolute accuracy, as the rocket orientation will be selected in real time via the ASCL Pitch-Yaw sequence. We suggest that $\pm 1 arcmin$ would be adequate. Roll orientation will be selected pre-launch, and no in-flight roll maneuvers are planned.

4.4 Pointing Strategy

The scientific objectives for this flight require the instruments to be pointed to several different locations in a solar active region. The method is identical to that used for 36.048, and is done in two stages. In the first, ASCL is used to point the instrument optic axes to one edge of a selected active region. This is accomplished with the aid of the on-board H-alpha system and the ASCL joystick. In the second stage, we will use a form of the ASCL linear scan sequence to define a series of three to five pointing positions along the active region. These positions are to be along a line defined by two successive points on the H-alpha image selected by the ASCL joystick. A series of images and spectra will be taken at each point under the control of the on-board computer. Synchronization of the ASCL pointing maneuvers and the on-board computer operation is done by means of a hand-shaking protocol between ASCL and the SPDE Ground Terminal that controls the RS-232 link.

The following sequence illustrates the operation:

1. Enable Pitch Yaw Sequence
2. Set Cross Hairs on desired active region location.
3. ASCL Transmits pointing commands.
4. Enable Linear Scan Sequence.
5. Set ASCL Cross-Hair to desired beginning of scan, enter coordinates.
6. Set ASCL Cross-Hair to desired end of scan, enter coordinates.

7. ASCL computes the coordinates of the five locations along the line joining the two points just selected.

8. ASCL transmits pointing commands (if required) to point the instruments at the first location.

9. ASCL signals SPDE Ground Terminal that pointing maneuver is done.

10. SPDE Ground Terminal transmits sequence-start command to on-board computer; monitors on-board computer status.

11. On-board computer makes a set of exposures; signals SPDE Ground Terminal when done.

12. SPDE Ground Terminal signals ASCL to move to next position.

13. ASCL transmits pointing commands for next position to SPARCS; signals SPDE Ground Terminal when done.

14. SPDE Ground Terminal transmits sequence-start command to on-board computer; monitors on-board computer status.

The last four steps are repeated until all positions have been observed. Details of the handshaking protocol between ASCL and the SPDE Ground Terminal are the same as for 36.048, assuming that the ASCL equipment is used. Implications of using the ASCL replacement system have not been assessed.

4.5 Launch Window Requirements

The Launch window will be determined by the following factors:

- There must be a suitable active region on the solar disk.
- The VLA (if available) should be observing the sun.
- The Prime ground based optical observatory should be in a favorable time zone for observing the sun with a reasonable chance of good seeing.
- The Yohkoh spacecraft must be in daylight, in the SAA-free portion of its orbit, and observing.

4.6 Success Criteria

4.6.1 Comprehensive Success Criteria

Comprehensive success criteria for this flight include the following:

- Successful launch and recovery.
- Acquisition of the sun by SPARCS.
- Successful operation of ASCL.
- 320 seconds of fine pointed observations above 80 km.
- One complete exposure sequence of an active region or flare with the DRSG system.
- One complete exposure sequence with the NIXI system.
- One complete exposure sequence with the UV imaging system.

4.6.2 Minimum Success Criteria

Minimum success criteria for this flight include the following:

- Successful launch and recovery.
- Acquisition of the sun by SPARCS.
- Successful operation of ASCL.
- 250 seconds of fine pointed observations above 80 km.
- One or more exposures of an active region or flare with one of the DRSG systems.
- One or more exposures with the NIXI system.
- One or more exposures with the UV imaging system.

4.7 Launch Criteria

The following are the Experimenter's Go / No–Go Launch Criteria:

- A suitable active region is present on the Sun.
- At least one ground based optical observatory is observing with good seeing conditions.
- The VLA (if available) is operating.
- Recovery aircraft are available to operate down range; weather is acceptable for their flights.
- All payload and rocket systems are operational.
- The RS-232 command link is operational.
- ASCL is operational.
- All Ground Support Equipment is operational
- At least one recent (less than 24 hours) image from the Yohkoh SXT instrument is available.

Appendix

A Instrument Technical Details

A New Sounding Rocket Payload
for
Solar Plasma Studies

A Reprint of
A Technical Paper Describing the SPDE Instrumentation

A New Sounding Rocket Payload
for
Solar Plasma Studies

Marilyn E. Bruner, William A. Brown
Kevin L. Appert
June, 1989

ABSTRACT

We have developed a new sounding rocket payload for the study of high temperature plasmas associated with solar active regions and flares. The payload includes a comprehensive set of instruments that will record both spectra and images in the UV, EUV and soft X-ray regions of the spectrum. Novel elements of the hardware include two new optical systems and a new structure that is based on a large optical table suspended within the payload cavity. The optical and mechanical components that make up each instrument are individually mounted to the optical table, reducing the overall system weight and ensuring that all instruments in the complement will remain co-aligned during launch. The optical table approach greatly reduces the development costs of new instruments, and makes for a very versatile system that can be quickly re-configured to meet new experimental objectives. The initial complement of instruments will include a 4 channel multilayer mirror Soft X-ray Imager, a Dual Range Stigmatic Spectrograph operating in the UV and EUV regions, the Transition Region Camera, (a high resolution ultraviolet filtergraph), and an H–α video imaging system. A stigmatic Flat Field Spectrographic operating in soft X-rays will be added following the first flight of the payload. All primary data are recorded on film. Sequencing of instrument operation is controlled by a small on-board computer that is directed in real time from a computer terminal on the ground. The ground terminal and the flight computer are connected via a full duplex serial communications link based on the RS232 standard, and on off-the- shelf hardware and software. The serial link also serves as a downlink for instrument and engineering status.

1 Introduction

The major thrust of our sounding rocket investigation is the determination of the physical conditions in solar flare and active region plasmas. It is based on a rich heritage of rocket and satellite research at Lockheed that has emphasized high resolution spectroscopy and imaging in the UV and Soft X-ray ranges. Our primary analysis tool is diagnostic spectroscopy applied to Soft X-ray, UV, and EUV spectra, guided by the analysis of Soft X-ray and UV images which give both geometric and radiometric boundary conditions. The essence of the analysis is straightforward. From the intensities of allowed transitions, we derive the emission measure, defined as the integral of the square of the electron density over the emitting volume. There are also a number of lines that are density sensitive in the sense that their intensities are not directly proportional to the emission measure, but have some other dependence. Both the emission measure and the electron density can be determined as functions of temperature by selecting appropriate ions. By combining the emission measure found in each temperature interval with the electron density determined for the same intervals we can derive the volume of the plasma that lies within each interval. This, together with the geometry, forms a fairly complete physical description of the plasma that can be compared with theoretical predictions. Since most of the plasma above a solar active region is confined by the magnetic field into a system of loops and arches, both the theoretical models and the observations will concentrate on the physics of these loop systems.

A key feature of the new payload is a large optical table provided with a pattern of tapped holes. Components of the various instrument systems are mounted on brackets that fasten to this hole pattern in much the same way that it is done in an ordinary ground-based laboratory. The instrument cluster can be quickly and inexpensively re-configured to meet new observing requirements. The cluster presently includes a dual range (UV and EUV) stigmatic spectrograph, an ultraviolet filtergraph, a normal incidence multilayer soft X-ray turret camera, and an H–α video imaging system. We plan to add a stigmatic flat-field soft X-ray spectrograph to the cluster during the next phase of our investigation. The payload fits within a 22 inch diameter by 120 inch long evacuable cylinder, and will be launched by a Terrier boosted Black Brant V rocket. During flight, the payload will be oriented by a SPARCS attitude control system. A real-time video image of the sun in the hydrogen alpha line, joystick control of the attitude, and the RS-232 serial link to the on-board computer will provide full interactive control of both target selection and instrument operation.

Exposure times for the spectrographs are expected to be of the order of seconds to tens of seconds. Thus, complete spatial coverage of a typical active region at full angular resolution is not possible during the few minutes of a rocket flight. Our strategy is to observe a series of loop cross sections, with the slit oriented roughly at right angles to the horizontal component of the magnetic field. The slit will be moved a few arc seconds between each position so that a series of parallel chord segments are observed. Since the spectrographs are stigmatic, each position will record a cross section of the loop system. During the analysis, the UV and X-ray images will be used to determine the loop geometry, indicating how the spectra should be interpolated between observed positions. The resulting data set is expected to be far more comprehensive than any that have been observed to date, and should help to resolve some of the remaining ambiguities in our current loop models.

2 The Optical Systems

2.1 The Dual Range Spectrograph (DRSG)

The Dual Range Spectrograph consists of an off-axis parabola operating as a prime focus telescope, a slit assembly, a toroidal grating assembly, and a film camera. Functionally, the DRSG operates as a stigmatic spectrograph. The primary mirror has a $1.8m$ focal length. The grating assembly contains two toroidal gratings, one optimized for the 1200 – 1400 Å region, and the other for the 265 – 304 Å region.

A discussion of the instrument may begin with the telescope primary. As shown in Figure 1, the primary mirror is a rectangular section cut from a paraboloid of revolution. The aspect ratio of the rectangular section is near 2:1, and defines two collecting areas. The lower collecting area is optimized for EUV reflectivity. The upper area is optimized for UV reflectivity and will be coated with a so-called "black mirror" coating to suppress visible light. Since they are part of the same parabolic surface, the upper and lower sections of the telescope primary have a common focus and the UV and EUV images are rigorously co-aligned on the entrance slit of the spectrograph. Note, however, that the chief rays, defined by lines from the center of each section to the center of the entrance slit, are not coincident, but converge toward the entrance slit, and then separate again inside the spectrograph, as shown in Figure 2 a. It is this feature of the telescope that allows the two sections of the spectrograph to operate simultaneously and independently. The projected slit length on the sun is about six arc minutes.

The upper grating in Figure 2a is ruled for the EUV, and is illuminated by the lower half of the primary mirror. It has a ruling frequency of 3600 grooves per millimeter and a nominal working distance of one meter. Use of the toroidal figure permits astigmatism to be substantially eliminated over the working wavelength range. The grating rulings are parallel to the plane of the drawing of Figure 2a and to the entrance slit, which lies in the plane of Figure 2a. The normal to the EUV grating is tipped down such that the chief ray strikes the grating at near-normal incidence. The plane of dispersion is perpendicular to the plane of Figure 2a and contains the chief ray. The spectrum is focused to one side of the entrance slit as shown in Figure 2 b, and directly behind the entrance slit as the slit is seen in Figure 2a. (The detector is shown above its actual location in this figure to avoid confusion in the ray diagram.) Note that the plane of dispersion is not parallel to the baseplate. The operating range of the EUV spectrograph extends from

This diagram shows how the rectangular primary mirror is derived as a portion of a full parabola of revolution. The two halves of the primary are coated differently, so that each half is optimized for its portion of the spectrum.

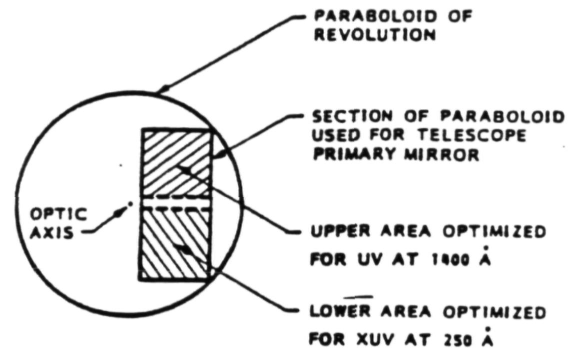

Figure 1: DRSG Primary Mirror

265 Å to slightly above 304 Å. The spectrograph provides internal image magnification of 1.1 so that the overall effective focal length of the instrument is $2m$.

The UV spectrograph section is essentially a mirror image of the EUV section. The toroidal UV grating is the lower one in Figure 2a, and its normal is tipped up, such that the chief ray from the upper section of the primary mirror is nearly perpendicular to the grating rulings. The plane of dispersion is, again, perpendicular to the plane of the drawing of Figure 2a, and contains the chief ray so that it is not parallel either to the baseplate or to the EUV dispersion plane. The spectral range of the UV section extends from 1200 Å to about 1420 Å in order to observe both the H–Lyman α line at 1216 Å and a group of several strong lines of Si IV, O IV, and S IV near 1400 Å that experience has shown to be very useful in deriving densities and emission measures at transition zone temperatures. The entire interval is rich in diagnostically useful lines formed at temperatures ranging from the temperature minimum to the impulsive phase of solar flares.

After leaving their respective gratings, the two chief rays cross behind the entrance slit so that the UV and EUV spectra are separated on the focal plane. This geometry also compensates for most of the focal plane tilt error resulting from the fact that the slit is not perpendicular to the chief ray of either spectrograph section. The EUV and UV dispersion planes form a dihedral angle whose vertex is a line perpendicular to the plane of Figure 2a, and passing through the center of the entrance slit. The residual tilt error in the design is only 0.3 degrees and results in a blur error of less than one micron at the focal plane of the f/20 system so that further correction is not necessary. The plane of the film is perpendicular to that of the baseplate. Ray tracings of the system have shown that the aberrations are well controlled; spot sizes are generally well below ten microns over the entire spectral and angular ranges.

2.1.1 Operation

As shown in Figures 2a and 2 b, light entering the instrument strikes the primary mirror which forms an inverted image of the sun on the entrance slit. The slit serves as a field stop, and defines a segment of a chord on the solar disk that will be sampled by the spectrograph sections. Light passing the slit illuminates the two gratings as previously discussed. The gratings, in turn, disperse the spectrum, and form images of the two spectral ranges on the film. Since both spectrographs are stigmatic, there is a one to one mapping of points along the sampled chord of the solar disk onto points along the length of the image of each spectral line. Thus for a given rocket orientation, the instrument simultaneously observes both the UV and the EUV spectra of about 500 spatial elements on the solar disk, assuming 12 micron pixels and a 10 arc minute long slit. This corresponds to an angular resolution of about 1.2 arcseconds.

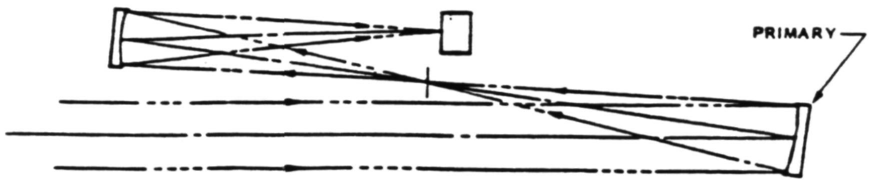

b) Top View

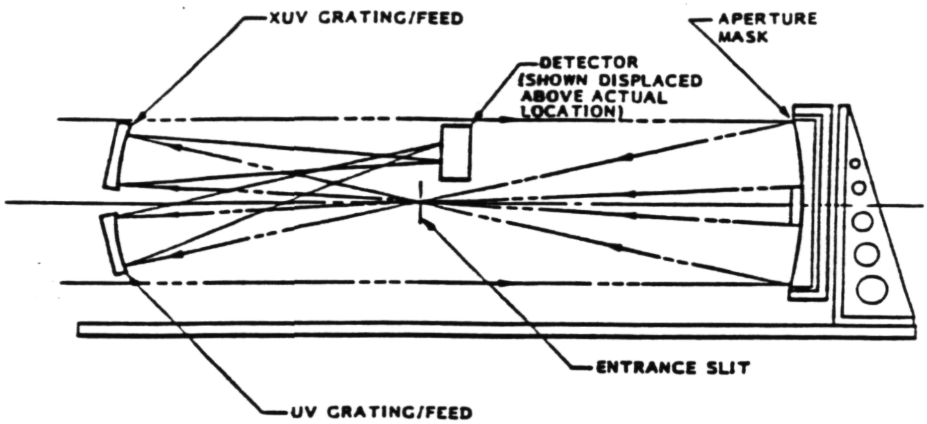

a) Side View

Figure 2: Dual Range Spectrograph Optics

2.2 The Flat Field Soft X-ray Spectrograph

This instrument is a stigmatic X-ray spectrograph that is to be added to the instrument complement during the next phase of the program. It covers a spectral range of 30 – 45 Å in first order, and 15 to 22.5 Å in second order. The optical design, shown in Figure 3 is an extension of the Rense – Violett [6] optical system using a varied-space grating. The design has been discussed by M. Chrisp[3], and further refined at Lockheed by S. Mrowka. As in the Rense – Violett system, light from the sun is collected by a toroidal mirror, which concentrates it on a slit located at its meridional focus. Light passing the slit is incident on a toroidal grating. The slit is located on the Rowland circle defined by the meridional radius of curvature of the grating. The sagittal radii of the collecting mirror and grating are chosen to approximately compensate for astigmatism near the center of the spectral range. The grating itself is holographically recorded using finite conjugate sources (i.e. point sources at finite distances from the grating vertex). The resulting grooves are curved and the groove spacing varies across the grating surface, both properties being determined by the wavelength and locations of the two sources used to form the interference pattern during recording.

The varied line spacing alters the focusing properties of the grating, since the angle of diffraction is now a function of position along the grating. With proper locations of the recording sources, the grating can be made to form the spectrum nearly at right angles to the exit beam, rather than along the Rowland circle as in a classical grating spectrograph. This has the effect of increasing the irradiance at the focal plane in comparison to the classical mount by a factor equal to the cosine of the angle of diffraction. The curvature of the rulings provides additional aberration correction. The system is stigmatic, giving both an additional increase in irradiance at the focal plane for a given source element, and a multiplex advantage

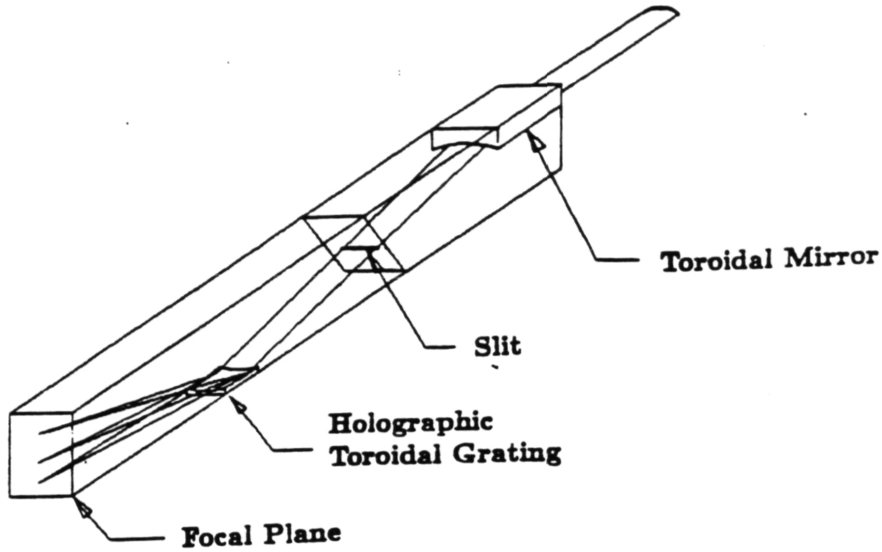

Figure 3: Flat Field Spectrograph Optics

in that many source elements can be observed simultaneously.

In the present design, good imaging is obtained over the wavelength ranges 30 to 45 Å in first order and 15 to 22.5 Å in second order, chosen to take advantage of the diagnostically useful lines in this part of the spectrum. The spectral resolution is about 0.02 Å, and a spatial resolution of about 2 arc seconds is maintained over a 1 arc minute long chord on the sun. Within its functional range, this design has an effective data collection rate that is over two thousand times higher than the Rowland circle instrument carried in our earlier flights [1].

2.3 The Normal Incidence Soft X-ray Imager

This instrument uses a series of four multi-layer mirrors to record soft X-ray images in selected lines between 44 Å and 304 Å. A multi-layer mirror [5,8,7,4]. consists of an ordinary mirror substrate that has been coated with alternating layers of two materials having widely differing atomic weights. The spacing of the layers is controlled to satisfy the Bragg equation for the wavelength of interest. The high Z layers act as partial reflectors, while the low Z layers serve as spacers. The resulting coating acts like an artificial Bragg crystal, and can have a substantial reflectivity, even at normal incidence. The maximum reflectivity increases with the number of layer pairs, and the width of the reflectivity peak is roughly equal to the central wavelength divided by the number of layers.

The four mirrors are spherical, and are mounted on a turret mechanism that rotates each mirror in turn into position as the primary mirror of a Herschelian telescope (See Figure 4). Images are recorded on Kodak T-max 100 film carried in a Canon Model T-70 35 mm camera body. Visible light is excluded by a thin metallic filter placed just in front of the film. The focal length of the system is 250 cm, and the expected angular resolution is about 1 arcsecond.

2.4 The UV Filtergraph

The Ultraviolet imaging system is a re-flight of the TRC (Transition region Camera) flown successfully on the four flights of our previous sounding rocket payload[2]. It consists of a 10 cm diameter

Cassegrainian telescope, followed by a filter wheel, shutter, and film camera. The Filtergraph uses interference filters to isolate four narrow bands in the 1200 to 2000 Å wavelength range. Images will be recorded on Kodak T-Max 100 film. The field of view covers the whole sun, and the angular resolution is better than 1 arc second.

2.5 The H–α Imaging System

This system consists of a ruggedized Questar telescope followed by a reticle and field lens assembly, a telecentric relay lens, an H–α filter, and a vidicon detector. It provides a real-time image of the sun during the flight, and is used in conjunction with the command link to select the fields to be observed with the spectrographs.

3 The Structural System

At the heart of any successful optical instrument, particularly one intended for space flight, is a sound structural–mechanical system. It must not only support the optical elements in their correct positions and orientations, but must maintain these alignments precisely throughout the rigors of the environmental testing and rocket launch environments. We have placed an additional requirement on the structural system for this payload; that it be easily and inexpensively modified as needed to meet new observing requirements as our scientific investigation develops. Our approach to achieving both goals is to base the structural system on a light weight optical table supported within the payload cavity, as suggested by Figure 4. The table is constructed of carbon fiber – epoxy composite face sheets bonded to aluminum honeycomb cores. It is in the form of an "I" beam, and is covered with a pattern of threaded inserts to which the optical components are mounted. The design of the face sheets is such that the coefficient of thermal expansion is quite small, desensitizing the system focus to temperature. In addition, a hydrophobic epoxy has been used so that the table will be dimensionally stable with respect to water vapor content.

The optical table is supported at the two ends by means of aluminum fittings bonded to the table material. One of these fittings contains a spherical bearing which constrains the end of the table rigidly with respect to the rocket, while allowing three degrees of rotational freedom. This bearing carries the payload's thrust load during launch. The fitting at the other end is fastened to the rocket via a flexible diaphragm that supports the end laterally and in torsion, but allows longitudinal motion to compensate for thermal expansion of the rocket cylinders. The diaphragm faces the sun during observations, and contains an aperture for each of the optical systems. This combination of constraints holds the table and its instrument complement securely in the payload compartment during the flight, but decouples it from any distortions of the rocket structure so that instrument alignment and performance is not compromised.

The payload is designed to be evacuated prior to launch so that water vapor and other residual contaminants will not affect instrument sensitivity. The payload compartment is fitted with a 3 inch diameter pumpout port so that it can be evacuated while mounted on the launcher. A motor operated door seals the aperture end of the payload during the pre-launch, ascent, and re-entry phases of the flight.

4 The Control Electronics

The operation of the payload is controlled by an off-the-shelf microcomputer, and contains a minimum of interface and other electronics. The computer controls sequencing of the UV Filtergraph, positioning of the X-ray Turret, and the opening and closing of the film camera shutters. Commands from the ground and engineering status from the instrument are relayed over a full-duplex RS-232 link. The software for the computer is written in FORTH. Since this payload will represent a pioneering attempt at

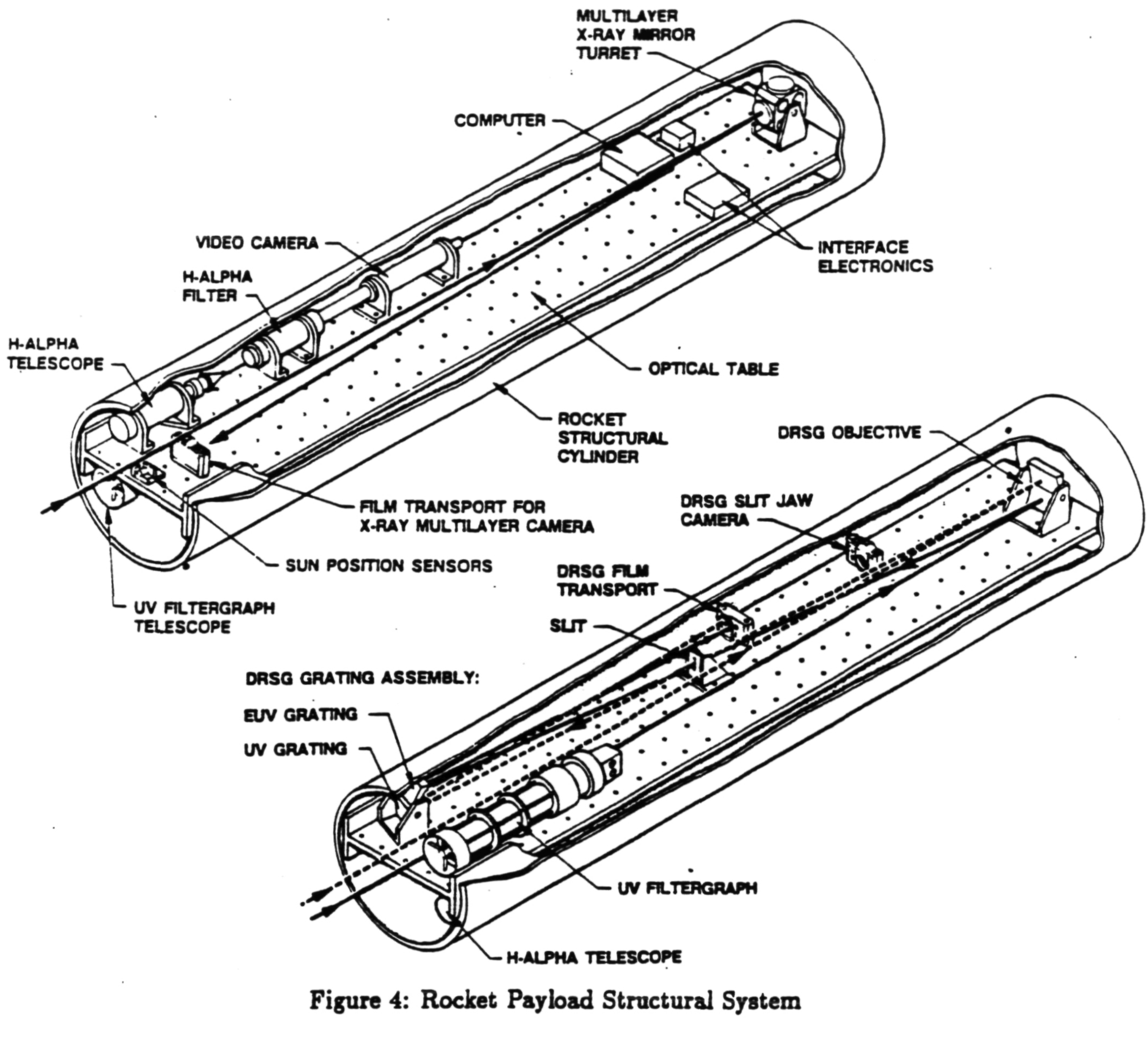

Figure 4: Rocket Payload Structural System

controlling an in-flight rocket payload via a real-time computer link, we will examine the system and its software in some detail.

The microcomputer consists of four printed circuit boards mounted to a common backplane. The first of these is a single-board computer with microprocessor, memory (RAM and ROM) serial ports, and timers. The remaining boards include a parallel port (for digital I/O), an analog data system (for temperature and voltage monitors) and a stepper motor clock. The boards all have the STD-bus form factor and pinout, but the connector is a military pin-and-socket type, rather than an edge connector. All boards except for the stepper motor clock are commercially available components.

Peripheral electronics include power conditioning, an interface electronics box for the UV Filtergraph, an interface and stepping motor driver for the X-ray turret, and a junction box. Signal conditioning circuits for the temperature sensors are also contained in the junction box.

4.1 Software

The software for the system is stored in non-volatile memory prior to launch. The microcomputer software consists of a scheduler, an engineering status acquisition module, and a communications handler. The software primarily does the job of scheduling events. Using one of a small selection of pre-defined observing sequences the motion mechanisms are moved and the camera shutters opened and closed at appropriate times. The selection and or modification of an observing sequence is either commanded from the ground, or a default is used in the event of communications failure. The implementation consists of an event manager which puts events on an event queue and the event handler which is invoked by the system clock interrupt and executes any event whose time has come. Events which must be accurately timed, such as film camera shutter openings and closings, are executed from the interrupt handler. Other events are implemented as tasks in a cooperative multi-tasker.

Engineering Status is acquired from temperature and position sensors distributed around the instrument. The communications handler maintains a dialog with the ground for the exchange of commands and engineering status information.

4.2 Serial Communications

Commands from the ground and engineering status from the payload are relayed via an RS-232 serial link. The RS-232 serial link is implemented using one of the serial ports on the microprocessor board. The interface is implemented as a three wire full duplex link, with no hardware handshaking. Flow control in a three-wire RS-232 link is handled by sending "stop" and "go" characters over the serial lines; however, in our implementation, the messages are appropriately sized and spaced so that flow control need not be implemented.

4.2.1 Blocks, Checksums, and Dropouts

The messages which are sent in an environment like the one we see in the rocket payload are subject to momentary disruptions in the link (dropouts). This makes it necessary to have some scheme to insure that commands arrive intact. The execution of a partial command or a garbled command is not acceptable, since it could compromise instrument operation. It is also necessary to detect the occurrence of such a dropout and re-send the command.

In order to accomplish this, the messages are sent to and from the rocket in groups of characters (blocks) with a checksum or cyclic redundancy code (CRC) at the end. The receiving end sends an acknowledgment if it receives the block intact. The blocks can be of fixed size or can contain a count so that the computer can know if some characters are missing.

Suppose, for example, that the computers have a dropout and lose a character from the middle of a message. The "end of block" and checksum will arrive, and the receiving computer will know something's missing. The recipient sends a "NAK" (not-acknowledged) and the block will be resent.

For another example, let's say the "end of block" is missing. Under those circumstances, the recipient waits for the end (the sender is not sending any more, as it is waiting for an ACK (acknowledgment). After a while, the receiver times out. This means that the computer looks at the timer and decides the block has taken too long, and that the "end of block" message must have been lost. The receiver then sends a NAK or a "timeout" message and the block is resent.

For a third case, consider what happens if all the characters arrive, but one or more of them are changed to different values. What will happen in this case is that the comparison of the CRC will fail, (this is not absolutely guaranteed, but is very, very likely) the receiving computer will send a NAK, and the block will be resent to it.

4.2.2 Link Loss

Another problem to be dealt with is a longer-term loss of the link. We are assuming two ground stations, and the possibility that the rocket will drift out of range of the active one, for example. At that point, the computer will count many time-outs and no complete blocks will be sent. After a suitable delay, the microcomputer will execute a stored default sequence until communication is re-established. The goal here is to provide some science data, however sub-optimal, in the event of catastrophic communications failure. In order to make detection of such a loss of the communications link possible, it is necessary to continuously send blocks in both directions, regardless of whether they contain useful information.

5 Acknowledgments

The authors are pleased to acknowledge the contributions of Mr. N. Didriksen, who did much of the mechanical design work, and to Mr. L. Yamanishi and Mr. R. Fujimoto, who worked on the electrical design. This work was supported by NASA under contract NAS5-29739.

References

[1] Bruner, et al., Opt. Eng. **19**, 433, (1980).

[2] Bonnet, R. M. et al, Astrophys. J., 237, L47, (1980).

[3] Chrisp, M. P., App. Opt. **22**, 1519, (1983).

[4] Henke, B. L., et al., Opt. Eng. **25**, 937, (1986).

[5] A number of papers describing recent work and containing references to earlier developments are contained in Proc. S.P.I.E. 563, (1985).

[6] Rense, W. A. and T. Violett, J. Opt. Soc. Am. **49**, 139, (1959).

[7] Sager, et al., J. Vac. Technol. A **4**, 641 (1986).

[8] Vinogradov, et al., Opt. Spectrosc. (USSR) **59**, 424 (1985).

C Experimenter's Flight Report

Lockheed Palo Alto Research Laboratory

3251 Hanover St.
Palo Alto, California
94304

Marilyn Bruner
Space Sciences Laboratory
91-30, Bldg. 252
(415) 424-3273

October 10, 1994

Mr. Larry J. Early
National Aeronautics and Space Administration
Goddard Space Flight Center
Wallops Flight Facility
Wallops Island, VA 23337-5099
Atten: 840

Dear Larry,

I am writing in response to your inquiry into the results from our recent Terrier-Black Brant sounding rocket mission, 36.123, launched from the White Sands Missile Range on April 25, 1994. We succeeded in recording a wealth of new solar data, both with the imaging systems and with the Dual Range Spectrograph. Scientifically the mission was unquestionably a success.

The new protective cover for the Normal Incidence X-ray Imager (NIXI) was successful in protecting the thin aluminum filter throughout the preparation, launch and recovery of the payload, and excellent images were recorded in the Fe IX and Fe XII lines. The re-designed mask system for the Dual Range Spectrograph was successful in reducing the scattered light level in the extreme ultraviolet channel, and in obtaining a better balance between the UV and EUV sections. The ultraviolet imaging system recorded excellent images in the hydrogen Lyman-α line, and one usable image in the C IV line.

The new EUV Imaging system that we had planned to test during this mission could not be completed within the available schedule and budget, and was deleted from the payload prior to its shipment to WSMR.

In evaluating the results against the Mission Success Criteria, it is clear that the Minimum Success Criteria were exceeded by a wide margin. The Comprehensive Success Criteria, stated in the Flight Requirements Plan dated 12 April, 1994 included the following:

a. Successful launch and recovery.

b. Acquisition of the sun by SPARCS.

c. Successful operation of ASCL.

d. 320 seconds of fine pointed observations above 80 km.

e. One complete exposure of an active region or flare with the DRSG system.

f. One complete exposure sequence with the NIXI system.

g. One complete exposure sequence with the UV imaging system.

Items a, b, and c were met, though with one reservation about the new Sparcs Command System (SCS), which was used in lieu of the ASCL for Mission 36.123. Our experience with the SCS will be discussed below.

Item d. was revised prior to launch as a result of an increased amount of ballast that was required to balance the payload. A new flight performance analysis on 19 April predicted 300 seconds of fine pointing above 80 km. In fact, the actual performance was 303 seconds. Thus the revised criterion d. was met.

Items e, f, and g, each called for the completion of at least one exposure sequence for the DRSG, NIXI, and UV imaging systems, respectively. Two out of a total of four planned exposure sequences were completed with each of these systems, satisfying these criteria. In my opinion, the Comprehensive Mission Success criteria were met; the mission was certainly successful in acquiring a valuable and scientifically useful data set.

There was one difficulty with the new SPARCS Command System (SCS) that caused an unfortunate delay in acquiring the desired target area on the sun. The difficulty arises from the small image scale and low contrast that is available on the new system, as compared to the old ASCL system that we have used in our prior flights. When the sun was acquired, the contrast and image brightness were such that no surface detail at all could be seen in the H-α image making it impossible to identify and select the target. In order to correct the problem, I had to shift my attention from the system trackball, open an auxiliary window with a mouse, and adjust brightness and contrast with software "sliders" on the screen. While this is not a particularly difficult procedure, it is slow and cumbersome, and caused a delay of many seconds before I could again turn my attention to identifying and selecting the target. We have recommended to the SPARCS project that they use a larger TV monitor for the image selection screen, and that its image controls (contrast, brightness, etc.) be implemented as analog controls with knobs that one can quickly adjust in an emergency.

A second difficulty originated in an error on my part in omitting one step in the commanding sequence. This step was to have moved a reference reticle so that it coincided with the crosshair in our guide telescope. This procedure was well developed on the ASCL system, and had been used successfully on many previous flights. Unfortunately, the SCS software did not behave the same way as the ASCL system and could not be used in the form in which we found it. Several iterations were made before arriving at a work-around that would be usable for the flight. There was no opportunity to practice with the final version of the software before the final countdown was under way, inviting the sort of error that occurred. This sort of problem is understandable, considering that Mission 36.123 represented the first use of the SCS for a solar experiment, and I'm confident that continued use of the system will make its use simpler and more reliable. Our recommendation here, is to make sure that the software does what the experimenter expects, and that it is ready well in advance to permit adequate training and practice before the launch.

There were two operational anomalies with the experiment sequence control system that occurred during the flight. On two occasions, the system paused at the end of the final exposure of a sequence and failed to advance to the next sequence. Each time, the system was re-started by ground command, using a recovery procedure that had been prepared for this purpose. We have not analyzed these anomalies in detail, but they are believed to have resulted from non-standard command procedures that were used by experiment team personnel in attempts to recover time lost during the acquisition phase.

This letter would not be complete without mentioning the excellent cooperation and support that we received from the skilled and highly professional crew that supported our mission. Without exception, we found them to be cheerful, helpful, energetic, and superbly competent. The continued high mission success rate that we have enjoyed over the years is due in large measure to these people and the dedication with which they approach each task. We are very fortunate to have such people available to us. I hope that you will pass my heartfelt thanks to all the members of the mission support staff, both at White Sands and at Wallops Island.

Sincerely yours,

Marilyn Bruner

Marilyn Bruner
Sr. Staff Scientist

D Subcontractor Reports

SOLAR PLASMA DIAGNOSTICS EXPERIMENT

DATA ANALYSIS

PROGRESS REPORT
PO SCZCZ1570 F

Period of Performance
June 16 through 30 July, 1995

W.A. Brown

1 INTRODUCTION

This report reports progress in research done under contract to Dr. M.E. Bruner the principal investigator of the SPDE program. The subject of the research is the study of the physics of the Solar Corona through the use of high resolution soft-x-ray and ultraviolet imagery and spectroscopy. A report covering the interval from April 26 to June 15 was submitted earlier and is appended here. Data from five flight instruments and two sounding rocket flights (1992 and 1994) is covered in the analysis. They are:

DRSG...Dual Range Spectrograph UV and EUV stigmatic spectra
TRC......UV filtergrams
H-alpha Video
NIXI imager for EUV lines
Slit Jaw camera of the DRSG

During this reporting period progress was made in these areas:

Relating absolute intensities in the UV spectrum of the DRSG with the TRC images.
Aspect solution relating pointing of the DRSG slit to the images obtained by the other instruments.

2 DRSG SPECTRA AND TRC IMAGES

Several new photometric scans of DRSG data were made. These improved on those made in '93 and '94 in that they revealed that the 1550 lines of C IV are not truly saturated in the spectra and can be used to estimate the absolute intensity of the solar flux. A case was worked out for the data array d1_240 which includes the one second exposure from the first pointing position of 36.048 from 1992. The Photometrics image was adjusted to include areas of clear film by taking a shorter Photometrics exposure (d1_60.pmi) of 60 msec duration to avoid overexposure of the clear film areas. From these two exposures of the long wavelength part of the spectrum (from 1393 to 1610 A) data files were made in terms of optical transmission. Photographic density was derived from this.

The conversion from density to log exposure followed Hoover's curve for 1215 Angstroms. To extend the result to 1550 A an observation of Fowler, Rense, and Simmons (AO 4 , p. 1596, 1965) was applied. This gave a relation for relative sensitivity from 1200 to 3500 A for early Schumann emulsions SWR and SC_5 processed in D-19. (For a given density the exposure required a given density is twice as high at 1500 as at 1200 A.)

A sample calculation was done as follows:
density of bright part of line (1548 A) 1.35
Film exposure to get this density = 2x10^9 photon/cm2
DRSG parameters at 1550 A

f# = 18
$R_g = 0.3$
$R_m = 0.7$

Solar radiance = exposure * $(f\#)^2/(.3 \times .7 \times 1) = 3 \times 10^{12}$ phot/cm^2/sec/sr

$$\text{Solar Radiance} = \frac{\text{exposure} * (f\#)^2}{(0.3 \times 0.7 \times 1)} = 3 \times 10^{12}\ \text{phot/cm}^2\text{/sec/sr}$$

This result may be compared with the intensity measured by the TRC using the C IV filter. For a bright part of the image the density is found to be about 0.8
This corresponds to a film exposure of 6×10^{7} photons per cm^2.

TRC f # = 24
exposure time = 1 sec
$R_m = 0.5$ for both mirrors
filter transmission = 0.002

Solar Intensity in the filter bandpass = 6×10^{13} phot/cm^2/sec/sr

3 ASPECT SOLUTION

The aspect solution relating DRSG slit positions to TRC images (and other images) was started. An outline of the project and the materials needed follows.

flights 36.048 , 12 May 1992
36.123 , 25 April, 1994

3.1. The goal is the localization of the projection of the DRSG slit on the solar disc.

3.2 Materials Needed:

3.2.1 TRC Images : C IV with limb, CN (no limb, no c IV lines), Lyman Alpha Images While the Lyman Alpha images are not as interesting in the study of the transition region plasma, the connection between DRSG line intensity and Lyman Alpha Image should be less ambiguous than for the long wavelength filter images. The Lyman Alpha filter transmits the H I line almost exclusively and thus the variations in intensity of Lyman Alpha along the spectral line should be exactly matched by those in the Lyman Alpha TRC image. This fit should then be useful in relating all other spectra to the solar disc.

3.2.2 Ground based H alpha image from time near flight time. We have the WSMR image for 1992(not sure we have the 1994 image by Charlie Welch.)

3.2.3 Rocket H alpha images captured from the onboard video. We have a set of these for 1992. This has not been done yet for the 1994 video data.

3.2.4 Rocket Slit Jaw Images. We have prints and Photometrics CCD images of the 1992 slit jaw images. (Negatives are missing). We have negatives and some Photometrics images for the 1994 data but no photographic enlargements except those originating in the Photometrics CCD image.

3.3 Measurements needed:

3.3.1 Angular tilt of DRSG slit with respect to H alpha features

3.3.2 Angular measurements of DRSG slit and relation to marks (scratch, etc.) on the slit surface.

3.4 Steps to reach Aspect Solution:

3.4.1 Find the distance in x,y from DRSG slit center to the sun center.
3.4.2 Find the angle between solar feature axes and DRSG slit

3.4.3 Discussion:

The x,y distance is different for each exposure. On the 1992 flight there were three pointing positions for spectra. In 1994 there were several more. The slit jaw camera images show the position of the slit with respect to the center of the solar disc. An arcsecond scale can be provided in the slit jaw camera images by using measured angular sizes of the scratch on the slit.

The angular reference will be found by a sequence of steps. The H-alpha image from the videos can be related to features in the ground based H-alpha images. These can be used to clarify the relation between the TRC images and the video h-alpha images.
On the video h-alpha images use the DRSG slit angle with respect to the h-alpha features.
Laboratory measurements of the h-alpha crosshair angle are used to relate to the DRSG slit direction.

4 RELATED WORK

During this period I had several discussions with John Hawley about the use of the Queensgate Etalon for UV narrow band filtering. We also discussed the alignment of the UV collimator and I demonstrated the use of the K&E theodolite and its application in verifying the collimation of the Mufaletto 36 inch collimator.

5 ATTACHMENTS

5.1 DRSG Line List with absolute intensities

5.2 DRSG Line intensity formula

5.3 H and D curves from Hoover paper for 1215 A on 101-7 film

5.4 Progress Report April through June 15th.

5 ATTACHMENTS

5.1 DRSG Line List with absolute intensities (see below)

5.2 DRSG Line intensity formula

W.A.B. rev. July 10, 1995

DRSG Line Intensities

This summary shows the connection between the DRSG spectrum and the photographic density in the line spectrum.

Consider first the exposure in photons of a piece of film. (The exposure is the quantity that is directly related to the photographic density.)

Define the solar line emission Φ with units ***photons/sec-sr-cmsq***

$$\textbf{EXPOSURE} = \Phi \times \Omega \times A_{sun} \times R_g \times R_m \times t \text{ (photons)}$$

Here Ω steradians is the solid angle subtended by the instrument (the DRSG here) and A_{sun} cmsq is the emitting area on the sun producing the density observed. R_g and R_m are the reflectivities of the grating and the mirror and **t** is the exposure time in seconds.

This expression can be put in terms of instrument variables as follows:

The solid angle of solar radiation collected by the DRSG is the collecting aperture divided by the square of the distance to the sun.

$$\Omega = A_{coll}/(D_{sun})^2$$

The telescope f/number, **f#**, the DRSG telescope focal length **fl** and the area on the film corresponding to **A_{sun}** are related by the geometric identity for similar triangles:

$$\frac{A_{sun}}{(D_{sun})^2} = \frac{\text{film area}}{fl^2}$$

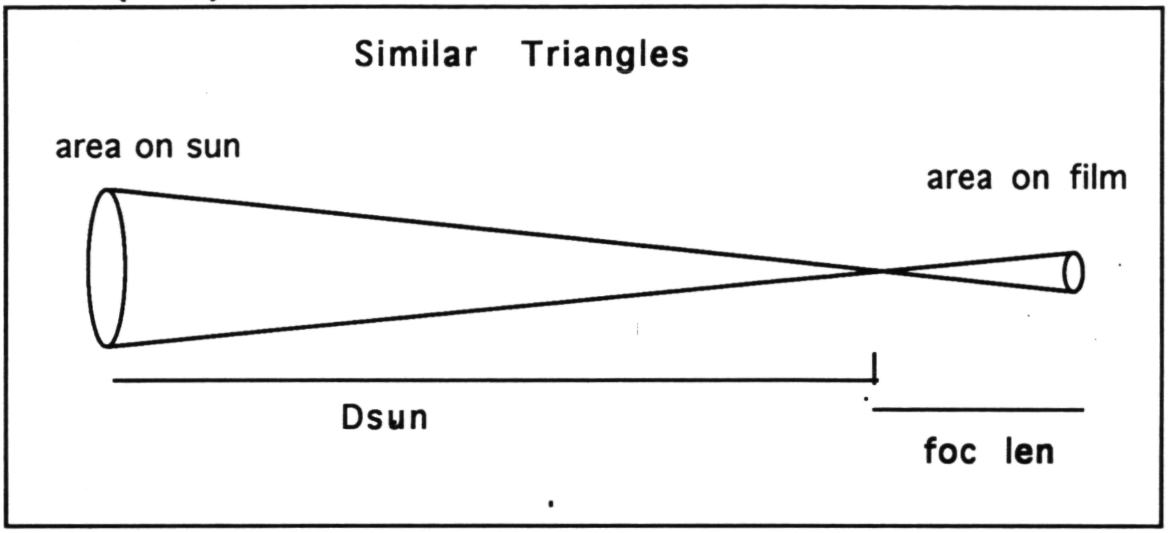

Now consider the term (Ω x A_{sun}) in the expression for **EXPOSURE** above:

$$(\Omega \times A_{sun}) = \frac{A_{coll}}{(D_{sun})^2} \times \frac{\text{film area} \times (D_{sun})^2}{fl^2}$$

We replace fl^2/A_{coll} by $f\#^2$ and cancel $(D_{sun})^2$ to get:

$$\text{EXPOSURE} = \frac{\Phi \times (\text{film area}) \times R_g \times R_m \times t}{f\#^2} \qquad \text{(photons)}$$

To simplify this we can further replace the total Exposure in photons with the exposure divided by the area considered.

Finally, the solar flux is expressed in terms of the observables:

$$\Phi = \frac{\text{Exposure (per unit area)} \times f\#^2}{R_g \times R_m \times t} \quad \text{photons/sec-sr-cmsq}$$

5.3 H and D curves from Hoover paper for 1215 A on 101-7 film

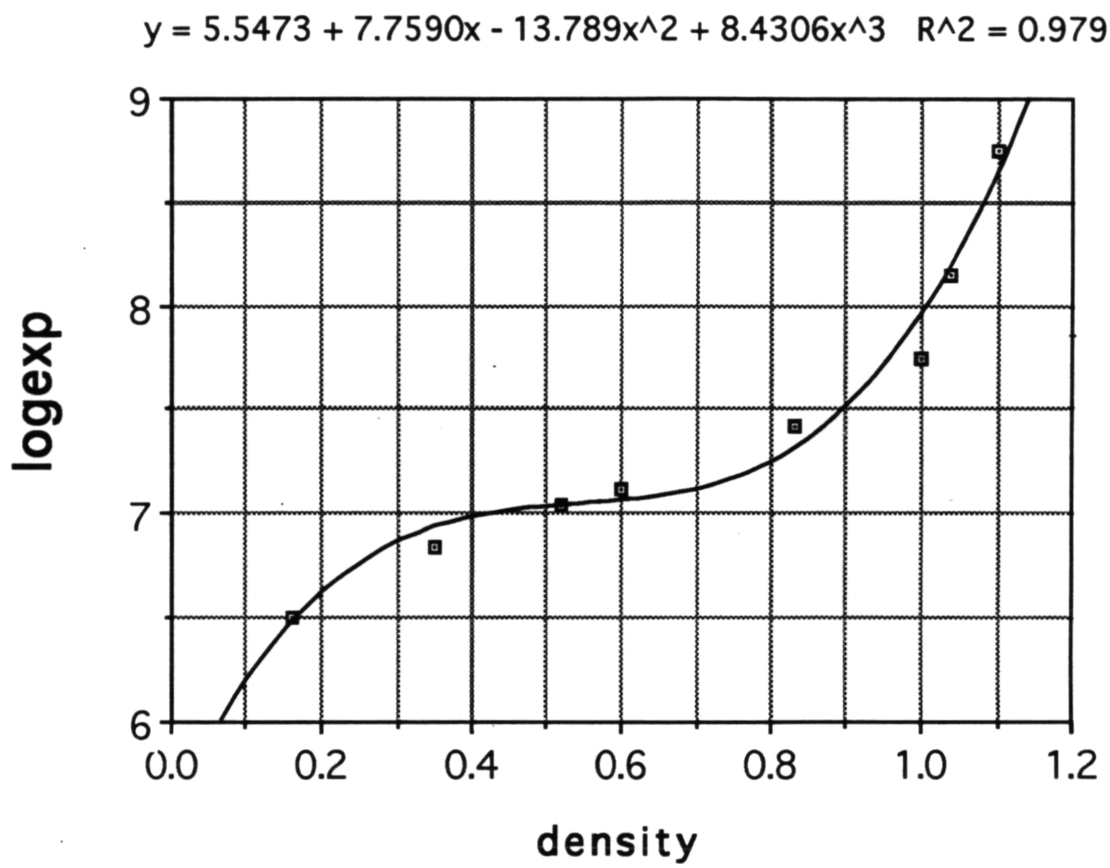

5.4 Progress Report April through June 15th.

This report summarizes the progress on work done under PO SCZCZ1570 F, dated 4-26-95.

The main effort has been in identifying the photographic results of the rocket experiments 36.048 and 36.123 which took place in 1992 and 1994. A notebook has been assembled which gathers together the materials available or provides information to identify computer files containing the material.

Film Log: Identifies 101-07 and XUV 100 film in the freezer and the flight instruments for which they were used. In some cases film remains on rolls used for flight.

Flight Film Index : A list of the flight exposures taken by cameras on the two SPDE flights. Includes exposure times, cross reference to computer files containing densitometer images, and NIXI bandpass identification. The handwritten table that follows is the result of an inspection of the flight films in our possession and some comments.

TRC Exposure times. For 36.048 the exposure times are gathered from the flight records.

Densitometer Data files. A list of the files on the UNIQ 386 computer (in the clean room) . Some of these files are on SXT2data0 hard disc.

DRSG line list from 36.048 This list contains only crude intensity information which should be used for identification only. Also useful for identification of the densitometer is the photographic enlargement and the appended scale.

Sample of DRSG spectra combining the files e1_lg4.pmi, e1_lg3.pmi, e1_lg2.pmi, and e1_long.pmi. Made from the 1992 data using the first or one second exposure these were the highest resolution digitized spectral images. Each of the four images represents only half of the available line length, to illustrate the overlapping of the data files.

Notes on the line spectra.

e-mail notes by Bruner, Damé, and Brown regarding the flight data from 1994

TRC image density comparison. This showed consistency between densities obtained by Damé using MAMA system and results from our PMI densitometry of Lyman Alpha images for the shortest Ly Alpha exposures on 36.048 and 36.123.

Work was done on understanding the relation between density and photographic exposure in DRSG, TRC, and NIXI images. Using the TRC comparison mentioned above, we can now put our own TRC images in the form of density maps. In the case of Lyman alpha images we can attach an exposure value. Difficulties in our own PMI densitometry were lessened by stopping the use of the fluorescent lamp for illumination of the light table. The AC lamp made short exposures useless so a new DC set-up is being employed.

Supported the visit of Luc Damé to this laboratory for discussions of TRC images. Discussed aspects of the data with B. Handy. Gave preliminary demonstration of the operation of the PMI densitometer set-up.

Wavelength	Ion	density Bkgnd	Density LINE	log Exposure Bkgnd	log Exposure Line+Bkgnd	Exposure Line Phot/cm2/sec	Solar Flux Phot/cm2/sec /sr
1215.7	H I	0.5	0.86	6.98	7.31	1.09E+07	1.68E+10
1264.7				5.50	5.50		
1302.2	O I	0.56	0.62	6.99	7.01	3.54E+05	5.46E+08
1304.8	O I	0.56	0.645	6.99	7.02	5.83E+05	8.99E+08
1306.0	O I	0.56	0.65	6.99	7.02	6.37E+05	9.84E+08
1309.3	Si II	0.56	0.59	6.99	7.00	1.53E+05	2.36E+08
1318.0				5.50	5.50		
1334.5	C II	0.57	0.81	7.00	7.20	5.80E+06	8.94E+09
1335.7	C II	0.57	0.84	7.00	7.26	8.30E+06	1.28E+10
1351.6				5.50	5.50		
1355.6				5.50	5.50		
1371.3				5.50	5.50		
1379.6				5.50	5.50		
1381.5				5.50	5.50		
1393.8	Si IV	0.65	0.925	7.02	7.52	2.25E+07	3.48E+10
1393.8	Si IV	0.6	0.87	7.00	7.34	1.17E+07	1.80E+10
1401.2	O IV	0.6	0.66	7.00	7.03	5.44E+05	8.39E+08
1402.8	Si IV	0.6	0.82	7.00	7.22	6.37E+06	9.83E+09
1404.0	O IV	0.6	0.602	7.00	7.00	1.27E+04	1.96E+07
1411.0				5.50	5.50		
1412.5				5.50	5.50		
1426.0		0.61	0.66	7.01	7.03	4.78E+05	7.37E+08
1442.0				5.50	5.50		
1445.0				5.50	5.50		
1452.0				5.50	5.50		
1454.8				5.50	5.50		
1468.0		0.65	0.76	7.02	7.11	2.53E+06	3.90E+09
1472.9		0.65	0.8	7.02	7.18	4.54E+06	7.01E+09

1474.0		0.65	0.78	7.02	7.14	3.42E+06	5.28E+09
1481.7		0.65	0.8	7.02	7.18	4.54E+06	7.01E+09
1483.0		0.65	0.76	7.02	7.11	2.53E+06	3.90E+09
1485.2				5.50	5.50		
1492.0				5.50	5.50		
1502.0				5.50	5.50		
1510.9	C II and N II	0.73	0.98	7.08	7.76	4.52E+07	6.97E+10
1526.7	Si II	0.72	0.96	7.07	7.66	3.43E+07	5.30E+10
1529.2				5.50	5.50		
1531.0				5.50	5.50		
1533.4	Si II	0.72	0.98	7.07	7.76	4.55E+07	7.02E+10
1537.4				5.50	5.50		
1541.0				5.50	5.50		
1542.0				5.50	5.50		
1544.0				5.50	5.50		
1545.3				5.50	5.50		
1548.2	C IV	0.7	1.08	7.05	8.37	2.21E+08	3.41E+11
1550.8	C IV	0.7	1.05	7.05	8.16	1.32E+08	2.04E+11
1555.0				5.50	5.50		
1559.1				5.50	5.50		
1560.5				5.50	5.50		
1561.2	C I	0.7	1.03	7.05	8.03	9.62E+07	1.48E+11
1564.0							
1566.8							
1568.0							
1570.0							
1573.5							
1574.7							
1577.0							
1578.4							
1580.5							
1584.8							
1588.0							

1590.4
1592.0
1594.5
1598.0
1600.0
1601.0
1602.5
1605.5
1607.0
1608.2
1611.0

SOLAR PLASMA DIAGNOSTICS EXPERIMENT

DATA ANALYSIS

FINAL REPORT
PO SCZCZ1570 F

Period of Performance
Aug. 7 through September 27, 1995

Wm. A. Brown

1 INTRODUCTION

This report reports progress in research done under contract to Dr. M.E. Bruner the principal investigator of the SPDE program. The subject of the research is the study of the physics of the Solar Corona through the use of high resolution soft-x-ray and ultraviolet imagery and spectroscopy. A report covering earlier intervals is contained elsewhere.

2 REVIEW OF DATA TASKS

The Statement of Work attached below structured the work in this effort into three parts. Broadly, these are the description of the existing data, evaluation of the need for further digitization and quantitative analysis on a subset of the data. An important part of the work was to be the transfer of knowledge regarding the SPDE data to Brian Handy and others and if possible the creation of scientific reports using the data. Not mentioned but very important is the relation of the SPDE data to the YOKOH and ground based data.

Earlier reports and verbal communications provided details of the data base as it now exists and the direction further work might take. These detailed the lists of the existing photographic materials and discussions on the nature and use of heterochromatic photometry. In 1994 certain parts of the photographic data were digitized for the purpose of getting a quick look at the material. This year closer study revealed inadequacies in the lighting used in the digitization and the presence of unnecessarily saturated digitizations. Many of these problems have been corrected and a procedure put in place to extract quantitative density data from the films.

We avoided embarking on a new effort in quantitative photometry using laboratory light sources, spectrometers and standard detectors although this will be essential if a research project requires more accurate determination of absolute radiances in spectra and images. A small supply of film exists to support such an effort. Our experience with this type of effort on the earlier XSST solar rocket program in the early eighties led us to caution in embarking until sufficient resources were available for completion. Some additional work on measurement of grating and mirror efficiency has been started by L. Shing in the laboratory.

3 OVERVIEW OF THE DATABASE

Information in the database has been organized by year of SPDE rocket flight. It includes:

Digitized photographic data for quick look assessment.
Photographic data converted to units of photographic density
Data converted to units of photon flux on film
Data converted to solar radiance
Lists of lines and identifications
Descriptions of the data
Descriptions and properties of the instruments on the rocket payload

The data is grouped into 1992 and 1994 sections and within each section grouped by instrument. The digitization of the TRC (UVI) data for 1992 was done by Luc Damé in France using the MAMA setup at the Institut D'Astronomie. All others were done in Palo Alto using Photometrics CCD and imaging software on a Lockheed furnished set-up which includes a 386 type PC.

4 Attachments

4.1 Revised Statement of Work April 24,1995

Contractor shall conduct a research program into the quantitative analysis of the photographic data obtained from the SPDE sounding rocket flights of May 1992 and April 1994.

Tasks Include:

1. Provide an itemization and qualitative description of the data obtained on flights 36.048 and 36.123
   Deliver Report on progress to Dr. M.E. Bruner 15 June 1995

2. Conduct an assessment of need for further digitization of sections of the photographic data, and provide instruction in this process.
   Deliver Report on progress to Dr. M.E. Bruner 30 July 1995

3. Perform quantitative analysis of selected portions of the data sets. Here emphasis will be on selected data sets leading to estimation of multitemperature emission measures. It is not anticipated thatnew laboratory investigations into heterochromatic photometry will be initiated into the characterization of the emulsions, although careful analysis might ultimately require this.
   Deliver Report on progress to Dr. M.E. Bruner 15 September 1995

This work will be performed by Dr. Wm. A. Brown at approximately half-time level with the final report to be delivered Sept. 15, 1995.

4.2 Informal Summary of Activities in August and September 1995

Work with John Hawley :
- Instruction in use of theodolite for collimator alignment
- Discussions of UV spectra and the monochromator
- Discussions of UV light sources

Work with B.N.H. in theodolite use for SPDE DRSG slit position.

Unpack and Pack SPDE payload (with K.A.).

Set up the payload to reproduce flight configuration, including replacement of gratings and NIXI mirrors into holders.

Met with Jean P. Weusler of UH to discuss FP interferometry and past rocket work.

Set up and used stable DC lamp for new digitization of DRSG and NIXI images.

Completed new photometric digitizations of all NIXI images from 36.123 (April1994)
Converted six images to photographic density files. These were the Fe XII 195 A images and the Fe IX 171 images of 1, 3, and 7 seconds exposure. Raw data and density images are stored in /2p/brown/nixi on SXT2

Some editorial work on the report covering the previous reporting period was done in the latest reporting period. Part of this involved reformatting and incorporating earlier data and revising tabular data.

E Flight Data Archive

This section will briefly describe the SPDE data archive that accompanies this Final Report. Contained in the archive are the original densitometry files from the flight film, image files from the coordinated ground-based observing campaign and from the Yohkoh SXT, observing logs for both flights, and utility software for accessing the files. The archive also contains pertinent documentation, and some photos of the instrumentation. The archive is in the form of a CD-ROM, which should be accessible either from UNIX-based or DOS based platforms.

The SPDE data archive is organized in an intuitive format, illustrated on the following page. The top level directories are divided into the two data directories ("1992" and "1994"), "software" for data analysis, instrument documentation and photographs. Each data directory is further broken up into the various instruments on the SPDE rocket payload and all ground-based and space-based observatories. Directories are further broken up for various wavelengths where appropriate. At a glance through the tree it is clear what data are available for a given rocket flight. It is hoped that the CD-ROM data archive will prove to be a useful addition to this printed report.

SPDE
Archive Directory Tree

```
\CDROM ──┬── software
         │
         ├── 1992 ──┬── uvi ──┬── civ
         │          │         ├── ctn
         │          │         └── lya
         │          │
         │          ├── drsg ──┬── uv
         │          │          └── euv
         │          │
         │          ├── slit_jaw
         │          │
         │          ├── obs_logs
         │          ├── yohkoh
         │          ├── la_palma
         │          ├── vla
         │          ├── kitt_peak
         │          └── big_bear
         │
         ├── 1994 ──┬── uvi ──┬── civ
         │          │         └── lya
         │          ├── nixi ──┬── 195a
         │          │          └── 171a
         │          ├── drsg ──┬── uv
         │          │          └── euv
         │          ├── slit_jaw
         │          ├── yohkoh
         │          ├── kitt_peak
         │          ├── mees
         │          └── obs_logs
         │
         ├── documentation
         │
         └── instrument
```

Revision Level: A
28-Sept.-1995
Brian Handy
Marilyn Bruner

Report Documentation Page in Lieu of NASA Form 298

1. Agency Use Only

2. Report Date
9/28/95

3. Report Type and Dates Covered
Final (Technical); September 1995

4. Title and Subtitle
Solar Plasma Diagnostic Experiment

5. Funding Numbers
NAS5-32147

6. Author
Marilyn E. Bruner

7. Performing Organization Name and Address
Lockheed Palo Alto Research Laboratories
Org. 91-30, Bldg. 252
3251 Hanover Street
Palo Alto, CA 94304

8. Performing Org Report No.

9. Sponsoring/Monitoring Agency Name & Address
NASA, GSFC Wallops Flight Facility
Wallops Island, VA

10. S/M Agency Report No.

11. Supplementary Notes

12a. Distribution/Availability Statement
Unclassified/Unlimited

12b. Distribution Code

13. Abstract (Maximum 200 Words)

This contract covers a sub-orbital research effort directed to the study of the physics of the solar corona throught the use of high resolution soft x-ray spectroscopy and high resolution ultraviolet imagery. The scope of this contract includes the modification of an existing sounding rocket payload, support of one launch field trip, data reduction and analysis, and reporting of the results to the scientific community.

14. Subject Terms
Solar Physics, Coronal Heating, Ultraviolet, X-rays, Sub-orbital

15. Number of Pages
73

16. Price Code

17. Security of Report	18. Security of Page	19. Security of Abstract	20. Limitations
Unclassified	Unclassified	Unclassified	None

Report Documentation Page in Lieu of NASA Form 1626

1. Report No. A	**2. Gov't Accession No.**	**3. Recipient Catalog No.**
4. Title and Subtitle **Solar Plasma Diagnostic Experiment** (SPDE) Final (Technical) Report		**5. Report Date** September 28, 1995
		6. Performing Organization Org. 91-30
7. Author Marilyn E. Bruner		**8. Perf. Org. Report No.**
9. Performing Organization Name and Address Org. 91-30, Bldg. 252 Lockheed Palo Alto Research Laboratories 3251 Hanover Street Palo Alto, CA 94304		**10. Work Unit No.** **11. Contract or Grant No.** NAS5-32147
12. Sponsoring Agency Name and Address NASA, GSFC Wallops Flight Facility Wallops Island, VA 23337		**13. Report Type & Period** Final (Technical) September 28, 1995
		14. Sponsoring Agency Code 244.3/603
15. Supplementary Notes		

16. Abstract

This contract covers a sub-orbital research effort directed to the study of the physics of the solar corona throught the use of high resolution soft x-ray spectroscopy and high resolution ultraviolet imagery. The scope of this contract includes the modification of an existing sounding rocket payload, support of one launch field trip, data reduction and analysis, and reporting of the results to the scientific community.

17. Key Words (by Author)	**18. Distribution Statement**		
Solar Physics, Coronal Heating, Ultraviolet, X-rays, Sub-orbital	Space Sciences, Solar Physics		
19. Security of Report	**20. Security of Page**	**21. No. of Pages**	**22. Price**
Unclassified	Unclassified	73	

For sale by the Superintendent of Documents, U.S. Government Printing Office, Washington, D.C. 20402